

Published in final edited form as:

J Med Chem. 2011 October 13; 54(19): 6843–6858. doi:10.1021/jm200794r.

N-O Chemistry for Antibiotics: Discovery of *N*-Alkyl-*N*-(pyridin-2-yl)hydroxylamine Scaffolds as Selective Antibacterial Agents Using Nitroso Diels-Alder and Ene Chemistry

Timothy A. Wencewicz, Baiyuan Yang, James R. Rudloff, Allen G. Oliver, and Marvin J. Miller*

Department of Chemistry and Biochemistry, 251 Nieuwland Science Hall, University of Notre Dame, Notre Dame, IN 46556, USA

Abstract

The discovery, syntheses, and structure-activity relationships (SAR) of a new family of heterocyclic antibacterial compounds based on *N*-alkyl-*N*-(pyridin-2-yl)hydroxylamine scaffolds are described. A structurally diverse library of ~100 heterocyclic molecules generated from Lewis acid-mediated nucleophilic ring opening reactions with nitroso Diels-Alder cycloadducts and nitroso ene reactions with substituted alkenes was evaluated in whole cell antibacterial assays. Compounds containing the *N*-alkyl-*N*-(pyridin-2-yl)hydroxylamine structure demonstrated selective and potent antibacterial activity against the Gram-positive bacterium *Micrococcus luteus* ATCC 10240 (MIC₉₀ = 2.0 μM or 0.41 μg/mL) and moderate activity against other Gram-positive strains including antibiotic resistant strains of *Staphylococcus aureus* (MRSA) and *Enterococcus faecalis* (VRE). A new synthetic route to the active core was developed using palladium-catalyzed Buchwald-Hartwig amination reactions of *N*-alkyl-*O*-(4-methoxybenzyl)hydroxylamines with 2-halo-pyridines that facilitated SAR studies and revealed the simplest active structural fragment. This work shows the value of using a combination of diversity-oriented synthesis (DOS) and parallel synthesis for identifying new antibacterial scaffolds.

Introduction

The development of bacterial resistance to current antibacterial chemotherapies is one of modern medicine's most important problems.^{1–3} The situation is confounded by a complex balance of medical, ethical, social, political, and economic factors all resulting in a decline of antibiotic development and rise in antibiotic resistance.⁴ With only a few last resort drugs available, such as vancomycin and linezolid, for treating highly resistant Gram-positive bacterial infections, there is a desperate need for new antibacterial agents based on new molecular scaffolds with novel modes of action.⁵ Historically, the antibiotic arms race has been maintained through the diligent work of medicinal chemists synthetically tailoring

*To whom correspondence should be addressed. M.J.M.: phone, (574) 631-7571; fax, (574) 631-6652; mmiller1@nd.edu.

Supporting Information Available

Complete list of compounds subjected to biological testing (Table S1). Complete list of biological data collected during this study (Table S2). Complete list of strains, markers, and origins for microorganisms used in this work (Table S3). Experimental procedures for the preparation of unpublished compounds not given in main article text. Copies of ¹H-NMR and ¹³C-NMR spectra for all unpublished compounds (9, 11a, 12, 14, 16, 18a–i, 19a–c, 27, 28c–i, 29a–i, 30a–i, 31a–i, 33–40a). Copies of HPLC chromatograms for compounds subjected to biological testing (7a, 7b, 9, 11a, 12, 14, 16, 18a–i, 19a–c, 30a–i, 31a–i, 32–40a). Crystal data, images of unit cell, and tables of atom coordinates and thermal parameters for the X-ray diffraction analysis of compound 40a. This material is available free of charge via the Internet at <http://pubs.acs.org>. CCDC 824255 contains the supplementary crystallographic data for this paper. These data can be obtained free of charge from The Cambridge Crystallographic Data Centre via www.ccdc.cam.ac.uk/data_request/cif.

existing antibacterial scaffolds to keep one step ahead of developing microbial resistance. The evolution of β -lactam antibiotics into many useful generations is the best example of this method.^{5,6} Modification of existing scaffolds is still the primary strategy of antibiotic resistance management employed today,⁷ but time is running out, the antibiotic pipeline is depleted, and a more long-term approach to managing antibiotic resistance is essential to regaining our medicinal advantage.

One promising approach to managing resistance involves identifying and developing new small molecules⁸ that hit new antibacterial targets and do not develop cross resistance with antibiotics acting on existing antibacterial targets.⁹ This approach is challenging since accessing such novel targets will likely require screening new molecular scaffolds that have not been isolated from nature or chemically synthesized. Existing compound libraries suffer from low structural novelty^{5,10,11} and often favor compounds with physical properties suitable for accessing eukaryotic cellular targets,⁵ while prokaryotes require different physiochemical properties for cell penetration.^{12,13} Modern medicinal chemistry techniques including fragment-based drug discovery (FBDD^a),^{14,15} computational structure-based design methods,¹⁶ high-throughput screening (HTS),¹⁷ and other target-based genomic approaches have been validated for identifying antibacterial compounds with new biological targets by the so called reverse chemical genetic approach.¹⁸ Overall, these methods alone have proven difficult to translate into well established whole cell antibiotic susceptibility assays due primarily to cell permeability issues. Additionally, most compound libraries used for virtual and *in vitro* screening lack the structural diversity for exploring unique chemical space.¹⁹

Traditional combinatorial library synthesis and HTS continue to play an important role in drug discovery, but have yielded limited success in bringing new chemical entities, including antibacterials, to market.²⁰ This lack of success is often attributed to the lack of structural diversity found in combinatorial compound libraries.^{19,20} Diversity-oriented synthesis (DOS) has emerged as an important strategy for producing structurally diverse and unbiased collections of small molecules covering unique chemical space.^{21,22} The use of DOS has already contributed to the discovery of new antibacterial scaffolds using whole cell HTS assays by the so called forward chemical genetic approach.^{18,23} Inclusion of DOS into antibacterial discovery programs provides a valuable source of structurally diverse molecular scaffolds for target-blind, unbiased screening.²³

Our group recently published new synthetic methodologies for the syntheses of highly functionalized hydroxylamine-containing compounds using Lewis acid-mediated nucleophilic ring opening reactions of nitroso Diels-Alder cycloadducts with alcohols^{24,25} and nitroso ene reactions with substituted alkenes.²⁶ These methodologies were an extension of our Modular Enhancement of Nature's Diversity (MEND) natural product derivatization program into a DOS strategy for rapidly producing structurally complex small molecules from simple starting materials.²⁷⁻³¹ Biological screening of the hydroxylamine-containing compounds revealed selective and potent antibacterial activity against *Micrococcus luteus* ATCC 10240 for compounds with pyridyl or isoxazole heterocycles. Discovery of the antibacterial activity coincided with a report from our group describing similar activity of

^aAbbreviations: Ac, acetyl; ATCC, American Type Culture Collection; BINAP, 2,2'-bis(diphenylphosphino)-1,1'-binaphthyl; Bn, benzyl; Boc, *tert*-butoxycarbonyl; CFU, colony forming unit; Cp, cyclopentadienyl; dba, dibenzylideneacetone; DMAP, 4-dimethylaminopyridine; DMF, dimethylformamide; DMSO, dimethylsulfoxide; DOS, diversity-oriented synthesis; DXR, 1-deoxy-D-xylulose-5-phosphate reductoisomerase; ESI, electrospray ionization; FBDD, fragment-based drug design; HPLC, high-performance liquid chromatography; HRMS, high-resolution mass spectrometry; HTS, high-throughput screening; IR, infrared; MEND, modular enhancement of nature's diversity; MEP, methylerythritol phosphate; MHII, Mueller-Hinton Media No. II; MIC, minimum inhibitory concentration; MRSA, methicillin-resistant *Staphylococcus aureus*; NMR, nuclear magnetic resonance; PG, protecting group; PMB, 4-methoxybenzyl; SAR, structure-activity relationship; TFA, trifluoroacetic acid; THF, tetrahydrofuran; TLC, thin layer chromatography; VRE, vancomycin-resistant *Enterococci*;

pyridyl-hydroxylamines derived from the ene reaction of 2-nitrosopyridines with the sesquiterpene natural product caryophyllene.³² Further literature searching revealed only one other report of *N*-alkyl-*N*-(pyridin-2-yl)hydroxylamines possessing moderate antibacterial activity against *Staphylococcus aureus* SG511, which also came from our group.³³ While other structurally unique hydroxylamine-containing antibacterial scaffolds are known (Figure 1),^{34–38} the novelty of the structures and obscurity of documented antibacterial activity inspired us to pursue this new antibacterial lead further.

Herein is described the discovery and elucidation of the structure-activity relationships (SAR) of a new class of Gram-positive selective antibacterial agents based on a *N*-alkyl-*N*-(pyridin-2-yl)hydroxylamine scaffold (Figure 1). Application of a DOS strategy using simple starting materials and the rich chemistry of nitroso Diels-Alder cycloaddition and nitroso ene reactions generated a structurally diverse library of oxyamino-containing compounds including hydroxamic acids, bicyclic oxazines, and *N*-alkyl-*N*-aryl-hydroxylamines (compounds **1–5**, Figure 2). The compounds were screened for biological activity in an unbiased, target-blind approach using whole cell antibacterial susceptibility assays. Nitroso ene reactions were used in a parallel synthesis strategy to explore SAR on the pyridine ring and the hydroxylamine side chain. A new convergent synthetic route was developed using palladium-catalyzed Buchwald-Hartwig cross-coupling amination reactions of *N*-alkyl-*O*-(4-methoxybenzyl)hydroxylamines with 2-halo-pyridines to achieve further SAR exploration. The simplest active fragment molecule was identified by synthesizing and testing all major molecular fragments. The discovery process outlined here highlights the combination of DOS and parallel synthesis as a useful strategy for identifying new antibacterial scaffolds (Figure 2).

Results and Discussion

Chemistry

The majority of molecules from the structurally diverse DOS library (compounds **1–5** generalized in Figure 2 and Table 4; exact structures as shown in the supporting information Table S1) were synthesized and characterized as described previously by our group using Lewis acid-mediated nucleophilic ring-opening reactions of nitroso Diels-Alder cycloadducts and nitroso ene reactions.^{24–26} Several important and highly biologically active compounds (**7**, **9**, and **11**) from this library were resynthesized according to the previously described methods (Scheme 1). Separable isomers **7a** and **7b** were prepared using an indium(III) triflate-mediated nucleophilic ring opening of 5-bromo-2-nitrosopyridine Diels-Alder cycloadduct **6** with methanol.²⁴ Compounds **9** and **11a,b** were synthesized using nitroso ene reactions with 2-methyl-2-butene and geraniol, respectively.²⁶ The major isomer from the ene reaction with geraniol (**11a**) was readily obtained in pure form by standard chromatographic methods, while the minor isomer (**11b**) was always isolated as a mixture with **11a**.

As described later, preliminary antibacterial data revealed that hydroxylamine compounds containing pyridine or isoxazole heterocycles showed strong antibacterial activity against *M. luteus* ATCC 10240, with pyridine being the preferred heterocycle. To confirm the preference for pyridine, compounds **12**, **14**, and **16** featuring pyridine, quinoline, and isoxazole heterocycles, respectively, with identical isoprenyl side chains were synthesized via ene reactions of the nitroso compounds with 2-methyl-2-butene (Scheme 2).

Nitroso ene chemistry was also used to rapidly synthesize a panel of substituted pyridine analogs with an isoprenyl side chain. Parallel reaction of 2-nitrosopyridine enophiles (**17a–i**) with 2-methyl-2-butene gave the corresponding racemic *N*-isoprenyl-*N*-(pyridin-2-

yl)hydroxylamines (**18a–i**; Table 1). These analogs were designed to probe SAR of the pyridine ring using substituents with differing electronics, sterics, and substitution patterns.

Nitroso ene chemistry was also used to generate a small panel of analogs that probed SAR of the hydroxylamine side chain. Reaction of 2-nitrosopyridine **10** with a variety of substituted alkenes gave the corresponding ene products (**19a–c**; Table 2). Compound **19a** has an α -methyl substituted isoprenyl side chain and is achiral. Compound **19b** lacks substitution and chirality at the carbon alpha to the hydroxylamine nitrogen and introduces a styrene unit. Compound **19c** retains the isoprenyl stereocenter and introduces a ketone into the side chain.

To probe deeper into the SAR and identify the simplest active molecular fragment, a new convergent synthesis of the general *N*-alkyl-*N*-(pyridin-2-yl)hydroxylamine scaffold was designed. The simplified core structure **20** was viewed retrosynthetically (Figure 3) by disconnecting the hydroxylamine bond at the 2-position of the pyridine ring. The C-N bond could be formed using Pd(0)-catalyzed Buchwald-Hartwig^{39,40} cross-coupling amination reactions of commercially available 2-halopyridines **21** with suitable *O*-protected hydroxylamines **22**. The *N*-substituted hydroxylamines **22** were available via *N*-alkylation of *N*-Boc-*O*-protected hydroxylamine **23** with alkyl halides **24** under S_N2 conditions followed by removal of the *N*-Boc protecting group with anhydrous acid.^{41,42} This synthetic route provided convergent access to the active core **20** where advanced functionality could be incorporated into both major fragments (**21** and **22**) separately.

An *O*-(4-methoxybenzyl)ether (PMB) protecting group was chosen for the hydroxylamine since PMB-ethers are easily removed by exposure to anhydrous acid.⁴³ The PMB-protected hydroxylamine derivative, *N*-Boc-*O*-(4-methoxybenzyl)hydroxylamine (BocNHOPMB, **27**) was synthesized on multigram scale (10.5 g) starting from *N*-hydroxyphthalimide (**25**) using a modified literature protocol (Scheme 3).^{44–46}

The target *N*-alkyl-*N*-(pyridin-2-yl)hydroxylamines were synthesized using a four step sequence starting from BocNHOPMB (**27**). Deprotonation of BocNHOPMB (**27**) with sodium hydride in DMF followed by S_N2 reaction with a variety of alkyl halides gave *N*-alkylated hydroxylamines **28a–i** in excellent yields. Brief exposure of compounds **28a–i** to anhydrous trifluoroacetic acid (TFA) selectively removed the *N*-Boc protecting groups and an aqueous NaHCO₃ wash gave the *N*-alkyl-*O*-PMB-hydroxylamines **29a–i** in good yields. The original aryl amination conditions reported by Buchwald and coworkers (Pd₂(dba)₃, (±) BINAP, NaO^tBu, toluene, 70 °C)⁴⁷ gave successful cross couplings of hydroxylamines **29a–i** with 2-bromopyridine yielding *N*-alkyl-*N*-(pyridin-2-yl)-*O*-PMB-hydroxylamines **30a–i**. Use of hydroxylamines **29a–i** in crude form gave the desired products, but chromatographic purification of the hydroxylamines prior to coupling improved yields. Increasing the size of the hydroxylamine alkyl substituent resulted in decreased cross-coupling yields following the trend hexyl (39%) < propyl (51%) < methyl (77%). The final deprotection of the PMB group under acidic conditions (TFA) in the presence of a cation scavenger (Et₃SiH) proceeded smoothly giving moderate to good yields (55–84%) of the desired *N*-alkyl-*N*-(pyridin-2-yl)hydroxylamine products (**31a–i**) after freebasing with aqueous NaHCO₃. The PMB-deprotection reactions were monitored closely since overexposure to TFA and Et₃SiH caused reduction of the *N*-*O* bond. The choice of Et₃SiH as a cation scavenger was important since other cation scavengers such as anisole led to decomposition of the products. The results from the four step synthetic sequence are summarized in Table 3.

The analogs generated from the Buchwald-Hartwig amination protocol were designed to investigate some key SAR points including the presence of a chiral center and allylic

unsaturation. A number of analogs with more drastic structural changes were also synthesized to address several other important SAR questions and identify the simplest active molecular fragment. To test the importance of the hydroxyl group an analog with the N-O bond reduced, *N*-benzylpyridin-2-amine (**32**), was prepared by subjecting compound **31d** to Pd-catalyzed hydrogenolysis. The *O*-acetyl analog (**33**) was prepared by treatment of **31d** with acetic anhydride (Scheme 4). Analogous N-O reduced (**34**) and *O*-acetyl (**35**) compounds were prepared from the more structurally complex compound **7b** (Scheme 4). Selective reduction of the N-O bond of compound **7b** was achieved using a titanium-mediated reduction procedure which gave analog **34** in good yield.⁴⁸ Acetylation of compound **7b** was achieved using acetic anhydride which provided analog **35** in excellent yield.

All the analogs presented thus far featured placement of the hydroxylamine at the 2-position of pyridine. The same Buchwald-Hartwig amination sequence discussed earlier was used to synthesize an analog with the hydroxylamine placed at the 3-position of the pyridine ring (compound **37**; Scheme 5). The Pd-catalyzed cross coupling of hydroxylamine **29d** was less effective at the 3-position of pyridine (compound **36**, 36% yield) relative to coupling at the 2-position (compound **30d**, 63% yield; Table 3), but still afforded the desired product (**36**). Deprotection of the PMB group with TFA/Et₃SiH and quenching with aqueous NaHCO₃ provided *N*-benzyl-*N*-(pyridin-3-yl)hydroxylamine (**37**).

The homologated analog **39** was designed to determine if direct attachment of the hydroxylamine to the pyridine ring was essential for activity. Alkylation of hydroxylamine **29d** with 2-(bromomethyl)pyridine gave *O*-PMB-protected hydroxylamine **38**. Removal of the PMB group with TFA/Et₃SiH gave the desired homologated analog **39** (Scheme 6).

As described later, preliminary testing indicated that nitroso ene reactions with geraniol generated highly antibacterially active compounds and that 6-alkyl substitution was favorable. Therefore, a 6-ethyl geraniol analog (**40a**) was synthesized via ene reaction of 6-ethyl-2-nitrosopyridine with geraniol (Scheme 7). The major isomer (**40a**) was isolated in pure form after chromatographic purification. A crystal of **40a** was obtained from CH₂Cl₂/hexanes and X-ray diffraction confirmed the structure of the major isomer (Figure 4; see supporting information for experimental details).

Biology

Selected compounds from the nitroso chemistry (compounds **1–5**, Figure 2)^{24–26} were compiled into a DOS library of ~100 small molecules with a high degree of appendage, functional group, stereochemical, and skeletal diversity.²³ The representative structural classes are given in Table 4. A complete list of exact structures is given in the supporting information (Table S1). The entire DOS compound library was screened against *Micrococcus luteus* ATCC 10240 using an in-house Kirby-Bauer agar diffusion antibiotic susceptibility whole cell assay (Table 4).^{49,50} The agar diffusion assay facilitated rapid identification of active compounds and comparison of relative potencies (increased size of the growth inhibition zone corresponds to an increase in potency; i.e., a lower minimum inhibitory concentration value).

The nitroso compounds and hydroxamic acids (**1**; Class A–C), bicyclic Diels-Alder cycloadducts (**2**; Class A–C), monocyclic hydroxamate-derived ring opened compounds (**3,4**; Class A), and acyclic hydroxamate derived ene products (**5**; Class A) were not active against *M. luteus*. The pyridyl and isoxazole ring opened compounds (**3,4**; Class B,C) and ene products (**5**, Class B,C) all showed strong antibacterial activity against *M. luteus* (Table 4). A complete list of biological data for all compounds is provided in the supporting information (Table S2).

In general, the *N*-alkyl-*N*-(pyridin-2-yl)hydroxylamines (**3**, **4**, and **5**; **Class B**) gave larger zones of growth inhibition in the agar diffusion assay than the *N*-alkyl-*N*-(5-methylisoxazol-3-yl)hydroxylamines (**3**, **4**, and **5**; **Class C**). The most active pyridyl compounds (**7a**, **9**, and **11a**) from the **Class B** *N*-alkyl-*N*-(pyridin-2-yl)hydroxylamines were selected for broader antibacterial testing against a panel of Gram-negative, Gram-positive, and yeast organisms, including antibiotic resistant strains of *S. aureus* (MRSA) and *E. faecalis* (VRE). The results of this broad antibacterial screening are summarized in Table 5 using a generalized scale to clearly show the narrow spectrum of antibacterial activity of compounds **7a**, **9**, and **11a**. Ciprofloxacin was included as a control antibiotic with known broad-spectrum activity.⁵¹

Compounds **7a**, **9**, and **11a** all displayed a similar narrow spectrum of antibacterial activity and the ciprofloxacin control (5 µg/mL in H₂O) showed broad spectrum activity against all strains except *M. luteus*. Compounds **7a**, **9**, and **11a** exclusively inhibited the growth of Gram-positive bacteria with particularly strong and selective potency against *M. luteus* ATCC 10240. The compounds showed comparable, although moderate, activity against both antibiotic susceptible (*S. aureus* SG511; *E. faecalis* ATCC 49532) and antibiotic resistant (*S. aureus* 134/94 MRSA; *E. faecalis* 1528 VRE) Gram-positive strains. Due to the highly selective antibacterial activity against Gram-positive organisms, *M. luteus* ATCC 10240, *S. aureus* SG511, and *E. faecalis* ATCC 49532 were used as model test organisms to evaluate SAR of the *N*-alkyl-*N*-(pyridin-2-yl)hydroxylamine analogs described from this point forward.

Two antibacterial susceptibility assays were used to evaluate the antibacterial activity of all the synthesized analogs, an agar diffusion assay^{49,50} and a visual end point broth microdilution assay.⁵² Data from the agar diffusion assay are reported as diameters of growth inhibition (mm) and data from the broth microdilution assay are reported as minimum inhibitory concentrations (MIC₉₀; µM). The fluoroquinolone antibiotic ciprofloxacin was included as a control.⁵¹ The results from the two assays are provided in Table 6.

The MIC₉₀ data for compounds **7a**, **9**, and **11a** mirrored the agar diffusion data and confirmed the selective potency against *M. luteus* (MIC₉₀ values of 4, 4, and 8 µM, respectively). Geranyl derivative **11a** also had a moderate MIC₉₀ of 64 µM against *S. aureus*. Similarly, analogs **12**, **14**, and **16** featuring pyridine, quinoline, and isoxazole heterocycles, respectively, all displayed selective antibacterial activity against *M. luteus*. The anti-*M. luteus* activity, based on MIC₉₀ values, of the heterocyclic cores increased in the order of isoxazole (64 µM) < quinoline (8 µM) = pyridine (8 µM), which confirmed the initial observation of pyridine as a favorable core.

The substituted pyridine analogs (**18a–i**) with identical isoprenyl side chains also preferentially inhibited the growth of *M. luteus* relative to *S. aureus* and *E. faecalis*. Methyl substitution at the 4- and 6-positions (compounds **9** and **18b**, respectively) enhanced anti-*M. luteus* activity (MIC₉₀ values of 4 µM) compared to the 3-position (compound **18c**) of the pyridine ring (MIC₉₀ value of 16 µM). There was a noticeable increase in potency in both assays for the 6-ethyl substituted compound (**18a**, 2 µM) compared to the unsubstituted (**12**, 8 µM) and 6-methyl substituted analogs (**9**, 4 µM). Halogen substitution (5-Cl, 5-Br, and 5-I) at the 5-position (compounds **18d–f**) of the pyridine ring also increased anti-*M. luteus* activity (MIC₉₀ values from 2–4 µM). 3,5-Dichloro substitution (compound **18g**) gave decreased anti-*M. luteus* activity (16 µM) relative to 5-chloro substitution (compound **18d**, 2 µM). Anti-*M. luteus* activity was not improved by the use of mixed alkyl-halogen substitution (5-Br-6-Me, **18h**; MIC₉₀ value of 4 µM) relative to monohalogen (5-Br, **18e**; MIC₉₀ value of 4 µM) or alkyl substitution alone (6-Me, **9**; MIC₉₀ value of 4 µM).

Substitution of the pyridine using 3-Cl-5-CF₃ substituents (compound **18i**) was detrimental (MIC₉₀ value of 128 μM against *M. luteus*). As supported by compounds **18c**, **18g**, and **18i**, any substitution at the 3-position of the pyridine ring resulted in decreased anti-*M. luteus* activity. Most of the analogs had no significant activity against *E. faecalis* or *S. aureus*, but the 4-methyl (**18b**) and 5-bromo (**18e**) derivatives showed a noticeable increase in activity against *S. aureus* relative to the other analogs. In general for the substituted pyridine analogs (**18a–i**), 5-halo and 6-alkyl substitution was favored for increased anti-*M. luteus* activity and the 6-ethyl analog (**18a**) emerged as the most potent compound in both assays (inhibition zone of 52 mm; MIC₉₀ value of 2 μM). The preference for 6-ethyl substitution was confirmed by the 6-ethyl substituted geranyl derivative **40a** which showed enhanced anti-*M. luteus* activity (MIC₉₀ value of 2 μM) relative to the unsubstituted geranyl derivative **11a** (MIC₉₀ value of 8 μM).

Evaluation of the pyridine analogs with differing hydroxylamine alkyl side chains (**19a–c**) showed that substitution of the hydroxylamine nitrogen is tolerated, but does noticeably influence the potency and selectivity. Compound **19a** had a gem-dimethyl isoprene unit and maintained strong potency against *M. luteus* (MIC₉₀ value of 4 μM) and weak anti-*S. aureus* activity (MIC₉₀ value of 128 μM). Compound **19b** featured a styrene side chain and showed decreased anti-*M. luteus* activity (MIC₉₀ value of 64 μM) and increased anti-*S. aureus* activity (MIC₉₀ value of 32 μM). Compound **19c** gave MIC₉₀ values of 16 μM against *M. luteus* and 128 μM against *S. aureus* which showed that an alkyl ketone was tolerated as a side chain. Antibacterial data from compounds **19a** and **19c** and the other unsubstituted pyridyl nitroso ene products **11a** and **12** showed that high substitution is tolerated on the alpha carbon of the isoprenyl hydroxylamine side chain. Data from compound **19b** indicated that alkyl substitution of the alpha carbon is important for enhancing the potency against *M. luteus* and that modification of the hydroxylamine side chain can enhance potency against *S. aureus*.

The *N*-alkyl-*N*-(pyridin-2-yl)hydroxylamine products **31a–i** from the Buchwald-Hartwig chemistry revealed some interesting SAR trends. Compound **31a** with a simple *N*-methyl side chain showed weak, but noticeable activity against *M. luteus*. This observation was important because compound **31a** represents the simplest active molecular fragment with all the critical structural components (pyridine heterocycle, N-OH at 2-position, and alkyl substitution of the hydroxylamine nitrogen). There was no drastic change in anti-*M. luteus* activity observed when the size of the alkyl side chain was increased from Me to Pr to *n*-hexyl (compounds **31a–c**). However, an *N*-benzyl group was found to be a suitable side chain and compound **31d** was the most active analog generated from the Buchwald-Hartwig chemistry against both *M. luteus* (MIC₉₀ value of 64 μM) and *S. aureus* (MIC₉₀ value of 128 μM). The benzyl derivative **31d** showed increased activity relative to the phenethyl derivative (**31e**) where the unsaturated carbon system was homologated. Compound **31f** had a simple *N*-allyl side chain and showed only weak anti-*M. luteus* activity in the agar diffusion assay.

The presence of an allylic unsaturated system appeared to be important for antibacterial activity and a benzyl side chain seemed to be a good choice especially since the phenyl ring offered a versatile point of derivatization. Preliminary SAR studies around the phenyl ring of benzyl derivative **31d** were performed using 3-phenoxy (**31g**), 4-trifluoromethyl (**31h**), and 4-trifluoromethoxy (**31i**) substituted compounds generated from the Buchwald-Hartwig cross-coupling chemistry. The phenyl substituted analogs were less active than the parent benzyl compound and the anti-*M. luteus* activity increased in the order of 3-(PhO)benzyl (**31g**) < 4-(CF₃)benzyl (**31h**) ≈ 4-(CF₃O)benzyl (**31i**) < benzyl (**31d**). Electron withdrawing groups appeared to be tolerated better than electron donating groups, but more data is needed to confirm this trend.

Comparison of the anti-*M. luteus* activity of allyl derivative **31f** (inhibition zone of 14 mm; MIC₉₀ value of >128 μM) to isoprenyl derivative **12** (inhibition zone of 31 mm; MIC₉₀ value of 8 μM) revealed a drastic difference in activity for only subtle differences in structure and molecular weight. The same trend was apparent when comparing all the simplified *N*-alkyl-*N*-(pyridin-2-yl)hydroxylamines **31a–i** to the unsubstituted pyridyl compounds with isoprenyl or substituted isoprenyl side chains generated from nitroso ene chemistry (**11a**, **12**, **19a**, and **19c**). The increased activity associated with the isoprenyl side chains must be attributed to substitution at the carbon alpha to the hydroxylamine or alkyl branching from the double bond, which are the only clear structural differences.

The scaffold SAR was expanded by evaluating compounds with more drastic structural modifications (**32–35**, **37**, and **39**). The *N*-O reduced analogs **32** and **34** had no antibacterial activity in both susceptibility assays. Additionally, testing of *O*-PMB protected compound **30d** revealed no antibacterial activity. These observations confirmed that the presence of the *N*-OH group is critical to activity. The *O*-acetyl analogs **33** and **35** had somewhat reduced activity against *M. luteus* (MIC₉₀ values of 128 μM and 32 μM, respectively) compared to the parent compounds **31d** and **7b** (MIC₉₀ values of 64 μM and 4 μM, respectively). The acetylated derivatives likely acted as prodrugs for the parent hydroxylamine compounds triggered by hydrolysis in the testing media. The 3-substituted pyridine analog **37** had reduced activity against *M. luteus* relative to 2-substituted pyridine analog **31d**. The homologated analog **39** showed no antibacterial activity. The anti-*M. luteus* data for compounds **37** and **39** suggested that *N*-arylation of the hydroxylamine is essential for activity and that *N*-arylation at the 2-position of pyridine is optimal.

Overall the agar diffusion data and the MIC₉₀ data in Table 6 correlated nicely. Compounds with the largest diameter growth inhibition zones (mm) in the agar diffusion assay gave the lowest MIC₉₀ values (μM) in the broth microdilution assay. Compounds with the *N*-alkyl-*N*-(pyridin-2-yl)hydroxylamine core structure had selectively potent activity against *M. luteus* (MIC₉₀ values as low as 2 μM) and weak to moderate activity against *S. aureus* (MIC₉₀ values as low as 32 μM). Although many compounds gave larger diameter zones of inhibition against *E. faecalis* compared to *S. aureus* in the agar diffusion assay, these zones were hazy and correlated to high MIC₉₀ values of >128 μM. Although the *N*-alkyl-*N*-(pyridin-2-yl)hydroxylamines only have weak to moderate activity against *S. aureus* and *E. faecalis*, the agar diffusion antibacterial data indicated that the compounds had comparable activity against antibiotic resistant strains (MRSA and VRE, Table 5). The SAR studies showed that the structure can be optimized to enhance activity against these clinically relevant Gram-positive pathogens. The SAR trends for anti-*M. luteus* activity of the *N*-alkyl-*N*-(pyridin-2-yl)hydroxylamines revealed in this study are summarized in Figure 5.

Representative compounds were also evaluated for growth inhibition of cancer cell lines (MCF-7, PC-3, and HeLa). None of the compounds showed significant toxicity towards the mammalian cell lines which indicated a potentially favorable therapeutic index. Experimental details and results from the anticancer assay are given in the supporting information (Table S2).

Further Discussion and Perspective

The selective antibacterial activity observed for the *N*-alkyl-*N*-(pyridin-2-yl)hydroxylamines against *M. luteus* was intriguing. While *M. luteus* is a commonly encountered Gram-positive bacterium that is part of normal human flora, it has a unique biochemistry^{53–55} and pattern of antibiotic susceptibility (nitrofurantoin and ciprofloxacin resistant).^{51,56} Consequently, *M. luteus* is commonly used in antibacterial screening programs to identify compounds with potential activity against resistant Gram-positive strains.⁵⁷ Beyond its use as a model

laboratory organism, *M. luteus* has clinical relevance as an infectious pathogen. While this bacterium was long considered nonpathogenic, recent literature recognizes *M. luteus* and other *Micrococci* as commonly misdiagnosed opportunistic pathogens that cause a variety of infections in immunocompromised patients that have been documented to be lethal in some cases.^{58,59} Clearly, *Micrococci* are clinically relevant pathogens that merit the development of new effective antibiotics especially since there is renewed interest in finding markets for species selective antimicrobial agents as a means of managing the development of resistance.^{5,60}

Initially it was suspected that the *N*-alkyl-*N*-(pyridin-2-yl)hydroxylamines might be acting as prodrugs for releasing a toxic nitroso compound inside of the bacterial cells⁶¹ or possibly generating reactive oxygen species from the aryl hydroxylamine.^{62,63} However, the parent nitroso compounds (**1**, **Class B,C**; Table 4) and Diels-Alder cycloadducts (**2**, **Class A–C**; Table 4), which can undergo retro Diels-Alder reactions to generate a nitroso species,⁶⁴ had no significant antibacterial activity. Additionally, establishment of clear SAR trends suggested the existence of a discrete, conserved cellular target. This hypothesis was also supported by the selective biological activity against Gram-positive bacteria, since a generally toxic molecule should show a broader spectrum of activity.

While any discussion of potential modes of action for these compounds is speculation at this point, some key structural features of the *N*-alkyl-*N*-(pyridin-2-yl)hydroxylamines showed striking similarities to known antibacterial compounds in the literature. The presence of a metal chelating group, the 2-pyridylhydroxylamine functionality,^{65,66} was similar to other known antibiotics containing N-OH bonds (Figure 1). For these known antibacterial agents, the N-OH bond played a key role by aiding in chelation of a metal in the active site of the target enzyme.^{34–37,67} Recent literature reports of fosmidomycin analogs^{68–71} revealed many structural similarities of *N*-alkyl-*N*-(pyridin-2-yl)hydroxylamines to known inhibitors (**41–44**) of 1-deoxy-D-xylulose-5-phosphate reductoisomerase (DXR) in the methylerythritol phosphate (MEP) isoprene biosynthesis pathway,⁷² a validated target for antibacterial agents (Figure 6).⁷³

The preference for isoprenyl and geranyl hydroxylamine side chains of the most active *N*-alkyl-*N*-(pyridin-2-yl)hydroxylamine analogs found in this work might aid in binding to enzymes along terpenoid biosynthetic pathways. This might explain the selective antibacterial activity of these compounds against *M. luteus* which is known to express high levels of terpenoid biosynthesis related enzymes in its cell membrane. Furthermore, *M. luteus* is known to possess a more promiscuous set of magnesium-dependent prenylation enzymes, relative to Gram-negative (*E. coli*) and other Gram-positive (*S. aureus*) strains.⁵⁵ Therefore, it is important to investigate these compounds for inhibition of isoprenoid and lipid biosynthetic pathways.^{73,74}

Summary and Conclusions

A DOS library of compounds was generated using nitroso Diels-Alder and nitroso ene chemistry which led to the discovery of *N*-alkyl-*N*-(pyridin-2-yl)hydroxylamine scaffolds as selective antibacterial agents against *Micrococcus luteus* ATCC 10240. The SAR was investigated using parallel synthesis with nitroso ene chemistry and a new Buchwald-Hartwig amination cross-coupling reaction of *O*-PMB-protected hydroxylamines with 2-bromopyridine. From these SAR studies the simplest active fragment molecule, *N*-methyl-*N*-(pyridin-2-yl)hydroxylamine (**31a**) was determined. New lead structures (**11a**, **18a**, **18d**, **31d**, and **40a**) were identified with potent activity against *M. luteus* (MIC₉₀ values as low as 2.0 μM) that will direct the production of future analogs. Structural similarities of *N*-alkyl-*N*-(pyridin-2-yl)hydroxylamines to known inhibitors of the MEP isoprenoid biosynthesis

pathway (**41–44**) have inspired the direction for future mode of action studies and the design of new analogs. This work demonstrated that an interdisciplinary combination of DOS, parallel synthesis, and whole-cell antibacterial susceptibility assays is an effective strategy for the discovery of new, structurally novel antibacterial scaffolds.

Experimental

Chemistry

General materials and methods—All reactions were performed under a dry argon atmosphere, unless otherwise stated. All solvents and reagents were obtained from commercial sources and used without further purification unless otherwise stated. Dichloromethane (CH₂Cl₂) was distilled from calcium hydride. Tetrahydrofuran (THF) was distilled from Na/benzophenone. Dimethylformamide (DMF), diisopropylethylamine (*i*Pr₂EtN), acetonitrile (CH₃CN), and triethylsilane (Et₃SiH) were used from Acros Seal[®] anhydrous bottles. All nitroso compounds were prepared from aminoheterocyclic precursors by a literature protocol⁷⁵ and were stored at –20 °C. Cycloadduct **6** was obtained from previous work published by our group.²⁴ Silica gel column chromatography was performed using Sorbent Technologies silica gel 60 (32–63 Zm). ¹H-NMR and ¹³C-NMR spectra were obtained on a 300 MHz, 500 MHz, or 600 MHz Varian DirectDrive spectrometer and FIDs were processed using ACD/ChemSketch version 10.04. Chemical shifts (δ) are given in parts per million (ppm) and are referenced to residual non-deuterated solvent. Coupling constants (*J*) are reported in hertz (Hz). High resolution, accurate mass measurements were obtained with a Bruker micrOTOF II electrospray ionization time-of-flight mass spectrometer in positive ion mode. Sample was introduced via flow injection at a rate of 4 μL/min, and mass spectra were accumulated from 50–3000 *m/z* for two minutes. X-ray diffraction analysis was performed on a Bruker APEX-II diffractometer (full experimental details and data processing are given in the supporting information). High-performance liquid chromatography (HPLC) was performed on a Waters 1525 Binary HPLC Pump instrument with a Waters 2487 Dual λ Absorbance Detector set at 254 nm operated by Breeze version 3.30 software. A YMC Pro C18 reverse phase column (3.0 × 50 mm) fit with precolumn frit (0.5 μm) and YMC Pro C18 guard column (2.0 × 10 mm) was used for all analyses. Mobile phases used were 10 mM ammonium acetate in HPLC grade water (A) and HPLC grade acetonitrile (B). A gradient was formed from 5%–80% of B in 10 min, then 80%–95% of B in 2 min, and then 95%–5% of B in 3 min at a flow rate of 0.7 mL/min (total run time of 15 min). Thin layer chromatography (TLC) was performed with aluminum-backed Merck 60-F₂₅₄ silica gel plates using a 254 nm lamp, aq. FeCl₃, aq. KMnO₄, or iodine vapor for visualization. Infrared (IR) spectra were recorded on a Bruker Tensor series FT-IR spectrometer using a diamond ATR accessory and signals are reported as wavenumbers in reciprocal centimeters (cm⁻¹). Melting points were determined in capillary tubes using a Thomas Hoover melting point apparatus and are uncorrected. The purity of compounds tested in biological assays was evaluated by analytical HPLC and verified to be ≥95%, unless otherwise noted.

(±) *N*-(5-Bromopyridin-2-yl)-*N*-((1*S*/*R*,4*S*/*R*)-4-methoxycyclohex-2-enyl)hydroxylamine (7a**) and *N*-(5-Bromopyridin-2-yl)-*N*-((1*S*/*R*,2*S*/*R*)-2-methoxycyclohex-3-enyl)hydroxylamine (**7b**)**—The synthesis of compounds **7a** and **7b** was replicated from work reported by Yang and Miller.²⁴ A solution of nitroso Diels-Alder cycloadduct **6** (103.0 mg, 0.39 mmol) in 3 mL of MeOH was treated with In(OTf)₃ (216.7 mg, 0.39 mmol) and heated to 70 °C (oil bath temperature). After 4 h, TLC (20% EtOAc in hexanes) showed complete consumption of starting material. The solution was cooled to rt and concentrated under reduced pressure. The resulting oil was partitioned between EtOAc (20 mL) and water (10 mL). The layers were separated and the water was

extracted with EtOAc (1 × 10 mL). The EtOAc layers were combined, dried over anhydrous MgSO₄, filtered, and concentrated. The crude product (~1:1 mixture of **7a**:**7b**) was purified by column chromatography (0.75 × 8 in silica gel; 10%–25% EtOAc in hexanes) to give isomer **7a** as an off-white solid (49.2 mg, 0.16 mmol), isomer **7b** as a clear, viscous oil (40.0 mg, 0.13 mmol), and a mixed fraction of **7a**/**7b** (20.0 mg, 0.07 mmol) as a clear, viscous oil (95% overall yield). (**7a**) HPLC retention time 6.86 min. (**7b**) HPLC retention time 7.32 min. All characterization data matched the previously reported data.²⁴

Typical procedure for nitroso ene reactions

(±) *N*-(6-Ethylpyridin-2-yl)-*N*-(3-methylbut-3-en-2-yl)hydroxylamine (18a**):** This procedure followed a general method reported previously.²⁶ 6-Ethyl-2-nitrosopyridine (**17a**; 271.0 mg, 1.99 mmol) was added as a solid to a solution of 2-methyl-2-butene (0.42 mL, 3.97 mmol) in 4 mL of anhydrous CH₂Cl₂ at 0 °C (ice bath temperature) and the solution turned orange. After 30 min, no starting nitroso compound (**17a**) was detected by TLC (20% EtOAc in hexanes). The solution was warmed to rt and the CH₂Cl₂ was evaporated under reduced pressure. The crude product was purified by column chromatography (1.25 × 7.5 in silica gel; 5%–30% EtOAc in hexanes) to give the desired ene adduct (**18a**) in 46% yield as a tan solid (190.0 mg, 0.92 mmol). Mp 64–65 °C; ¹H-NMR (600 MHz, DMSO-*d*₆) δ 8.68 (br s, N-OH, 1 H), 7.48 (dd, *J* = 8.2, 7.3 Hz, 1 H), 6.85 (d, *J* = 8.2 Hz, 1 H), 6.57 (d, *J* = 7.0 Hz, 1 H), 5.12 (q, *J* = 6.5 Hz, 1 H), 4.88–4.86 (m, 1 H), 4.84–4.82 (m, 1 H), 2.59 (q, *J* = 7.6 Hz, 3 H), 1.71 (s, 3 H), 1.18–1.15 (m, 6 H); ¹³C-NMR (150 MHz, DMSO-*d*₆) δ 162.5, 160.2, 146.1, 137.8, 112.2, 111.6, 105.8, 58.2, 30.5, 21.5, 13.7, 13.6; HRMS-ESI (*m/z*): [M + H]⁺ calcd. for C₁₂H₁₉N₂O: 207.1492, found 207.1488; IR (neat): 3139.7 (br), 3092.3, 1589.6, 1572.1, 1441.2, 1108.9, 968.9 cm⁻¹; HPLC retention time 8.34 min.

***N*-Boc-*O*-(4-Methoxybenzyl)hydroxylamine (BocNHOPMB, **27**):** This compound was prepared in 64% overall yield following a modified literature procedure.⁴⁴ *N*-Hydroxyphthalimide (10.53 g, 64.5 mmol), **25**, was treated with 4-methoxybenzyl chloride (8.9 mL, 65.4 mmol) and triethylamine (22.0 mL, 158.0 mmol), respectively, in 200 mL of DMF. The dark red solution was heated to 90 °C (oil bath temperature) for 1 h. The mixture was cooled to ~45 °C and poured over ice water. Product **26** precipitated as a light brown solid and was isolated via vacuum filtration and dried overnight under vacuum (12.99 g, 71%). ¹H-NMR (500 MHz, CDCl₃) δ 7.80–7.75 (m, 2 H), 7.73–7.68 (m, 2 H), 7.43 (d, *J* = 8.4 Hz, 2 H), 6.86 (d, *J* = 8.4 Hz, 2 H), 5.13 (s, 2 H), 3.78 (s, 3 H); ¹³C-NMR (125 MHz, CDCl₃) δ 163.4, 160.3, 134.3, 131.5, 128.7, 125.7, 123.3, 113.8, 79.4, 55.1. The solid was dissolved in 188 mL of DMF:MeOH (12:25) while at 60 °C (oil bath temperature) and treated with hydrazine hydrate (65% v/v; 7.0 mL, 146.5 mmol). After 10 min, the mixture was cooled to rt and diluted with 100 mL of H₂O. The MeOH was removed under reduced pressure and the DMF/H₂O mixture was extracted with EtOAc (4 × 100 mL). The combined EtOAc layers were dried over anhydrous MgSO₄, filtered, and concentrated to give 11.0 g of a faint, orange liquid. This liquid was immediately dissolved in 100 mL of THF:H₂O (1:1) and treated with triethylamine (6.5 mL, 46.6 mmol) and Boc anhydride (12.0 g, 55.0 mmol), respectively. After 2 h, the THF was removed under reduced pressure and the H₂O was extracted with EtOAc (2 × 50 mL). The combined EtOAc layers were washed with 5% aq. citric acid (1 × 25 mL) and water (1 × 25 mL), dried over anhydrous MgSO₄, filtered, and concentrated to give 14.7 g of a clear, orange liquid. Purification by column chromatography (3 × 6 in silica gel; 20% EtOAc in hexanes) provided the desired product (**27**) in 90% yield (2 steps) as a clear, colorless liquid (10.49 g, 41.4 mmol). ¹H-NMR (600 MHz, CDCl₃) δ 7.35–7.32 (m, 2 H), 7.07 (s, 1 H), 6.91–6.88 (m, 2 H), 4.80 (s, 2 H), 3.82 (s, 3 H), 1.49 (s, 9 H); ¹³C-NMR (150 MHz, CDCl₃) δ 159.8, 156.7, 130.8, 127.8, 113.8, 81.6, 78.0, 55.3, 28.2; HRMS-ESI (*m/z*): [M+Na]⁺ calcd. for C₁₃H₁₉NNaO₄: 276.1206, found 276.1202; IR (neat): 3285.8 (br), 1715.8, 1245.3, 1162.8, 1099.8, 1032.4 cm⁻¹.

Typical procedure for the alkylation of BocNHOPMB

***N*-Boc-*N*-Benzyl-*O*-(4-methoxybenzyl)hydroxylamine (28d):** Sodium hydride (60% in mineral oil; 400 mg, 10.00 mmol) solid was added to a solution of compound **27** (1.955 g, 7.72 mmol) in 20 mL of anhydrous DMF at 0 °C (ice bath temperature). The solution bubbled and turned faint yellow. After stirring for 30 min, benzylbromide (1.1 mL, 9.26 mmol) was added dropwise over 5 min and the mixture was warmed to rt. After 6 h, no starting material (**27**) was detected by TLC (10% EtOAc in hexanes). The off-white, opaque mixture was cooled to 0 °C and 10% aq. NaHCO₃ (10 mL) was added slowly. The DMF and H₂O were removed by high vacuum rotary evaporation (~1 mm Hg). The resulting slurry was partitioned between EtOAc (30 mL) and H₂O (30 mL). The layers were separated and the H₂O was extracted with EtOAc (1 × 30 mL). The EtOAc layers were combined, washed with brine (1 × 30 mL), dried over anhydrous MgSO₄, filtered, and concentrated. The crude product was purified by column chromatography (1 × 6 in silica gel; 10%–20% EtOAc in hexanes) to give the desired product (**28d**) in 99% yield as a clear, colorless liquid (2.64 g, 7.69 mmol). ¹H-NMR (600 MHz, CDCl₃) δ 7.38–7.28 (m, 5 H), 7.21–7.18 (m, 2 H), 6.87–6.84 (m, 2 H), 4.63 (s, 2 H), 4.55 (s, 2 H), 3.81 (s, 3 H), 1.52 (s, 9 H); ¹³C-NMR (150 MHz, CDCl₃) δ 159.7, 156.6, 136.9, 131.0, 128.7, 128.3, 127.7, 127.4, 113.7, 81.4, 76.8, 55.2, 53.9, 28.3; HRMS-ESI (m/z): [M+H]⁺ calcd. for C₂₀H₂₆NO₄: 344.1856, found 344.1851; IR (neat): 3064.4, 3033.1, 3003.0, 1697.9, 1247.4, 1157.1, 1089.4, 1032.2 cm⁻¹.

Typical procedure for the *N*-Boc-deprotections of *N*-Boc-*N*-alkyl-*O*-(4-methoxybenzyl)hydroxylamines

***N*-Benzyl-*O*-(4-methoxybenzyl)hydroxylamine (29d):** Anhydrous TFA (2 mL) was added slowly to a solution of compound **28d** (1.14 g, 3.32 mmol) in 8 mL of anhydrous CH₂Cl₂. The clear, colorless solution bubbled upon addition of TFA. After 15 min, the TFA and CH₂Cl₂ were evaporated under reduced pressure giving a clear, colorless liquid. This material was dissolved in CHCl₃ (25 mL) and washed with satd. aq. NaHCO₃ (1 × 50 mL). The CHCl₃ was separated, dried over anhydrous MgSO₄, filtered, and concentrated. The crude product was purified by column chromatography (1.25 × 6 in silica gel; 10%–20% EtOAc in hexanes) to give the desired product (**29d**) in 77% yield as a clear, colorless liquid (623.8 mg, 2.56 mmol). ¹H-NMR (600 MHz, CDCl₃) δ 7.38–7.28 (m, 5 H), 7.27–7.24 (m, 2 H), 6.89–6.86 (m, 2 H), 5.69 (br s, NH, 1 H), 4.60 (s, 2 H), 4.05 (s, 2 H), 3.81 (s, 3 H); ¹³C-NMR (150 MHz, CDCl₃) δ 159.3, 137.6, 130.1, 129.9, 129.0, 128.4, 127.4, 113.7, 75.9, 56.5, 55.2; HRMS-ESI (m/z): [M+H]⁺ calcd. for C₁₅H₁₈NO₂: 244.1332, found 244.1320; IR (neat): 3260.3 (br), 3062.0, 3030.5, 3001.4, 1611.0, 1511.7, 1244.7, 1031.9 cm⁻¹.

Typical procedure for the Buchwald-Hartwig amination cross-coupling reactions

***N*-Benzyl-*O*-(4-methoxybenzyl)-*N*-(pyridin-2-yl)hydroxylamine (30d):** This procedure followed a general method reported previously by Buchwald and coworkers.⁴⁷ Hydroxylamine **29d** (300.0 mg, 1.23 mmol), 2-bromopyridine (0.10 mL, 1.00 mmol), Pd₂(dba)₃ (18.0 mg, 0.02 mmol), (±) BINAP (25.0 mg, 0.04 mmol), and NaO^tBu (134.0 mg, 1.40 mmol) were dissolved in 9 mL of anhydrous toluene, respectively, in an oven-dried, argon-flushed Schlenk tube. The brown mixture was heated to 70 °C (oil bath temperature) overnight. The mixture turned darker brown over the course of the reaction. After 64 h, the mixture was cooled to rt, diluted with Et₂O (20 mL), and filtered through celite. The clear, orange solution was washed with brine (1 × 20 mL), dried over anhydrous MgSO₄, filtered, and concentrated. The crude product was purified by column chromatography (1 × 6 in silica gel; CH₂Cl₂ as eluent) to give the desired product (**30d**) in 63% yield as a clear, colorless liquid (201.2 mg, 0.63 mmol). ¹H-NMR (600 MHz, CDCl₃) δ 8.31 (ddd, *J* = 4.8, 1.9, 0.9 Hz, 1 H), 7.60–7.57 (m, 1 H), 7.46–7.44 (m, 2 H), 7.36–7.32 (m, 2 H), 7.32–7.28 (m, 1 H), 7.19–7.16 (m, 2 H), 7.10 (dt, *J* = 8.2, 0.9 Hz, 1 H), 6.87–6.85 (m,

2 H), 6.82 (ddd, $J = 7.3, 4.8, 0.9$ Hz, 1 H), 4.87 (s, 2 H), 4.56 (s, 2 H), 3.81 (s, 3 H); ^{13}C -NMR (150 MHz, CDCl_3) δ 162.4, 159.6, 147.8, 137.9, 137.6, 130.8, 129.7, 128.1, 128.0, 127.2, 116.3, 113.8, 109.2, 76.2, 57.4, 55.2; HRMS-ESI (m/z): $[\text{M}+\text{H}]^+$ calcd. for $\text{C}_{20}\text{H}_{21}\text{N}_2\text{O}_2$: 321.1598, found 321.1599; IR (neat): 3061.7, 3031.0, 3004.1, 1587.0, 1432.8, 1247.3, 1030.9 cm^{-1} ; HPLC retention time 9.78 min.

Typical procedure for the PMB-deprotection reactions

***N*-Benzyl-*N*-(pyridin-2-yl)hydroxylamine (31d):** Anhydrous TFA (3 mL) was added slowly to a solution of compound **30d** (100.0 mg, 0.31 mmol) and triethylsilane (0.10 mL, 0.63 mmol) in 7 mL of anhydrous CH_2Cl_2 . After 11 h, a small aliquot of the solution was quenched with satd. aq. NaHCO_3 and no starting material (**30d**) was detected by TLC (20% EtOAc in hexanes). The solution was diluted with CH_2Cl_2 (20 mL) and washed with satd. aq. NaHCO_3 (1×30 mL). The CH_2Cl_2 was separated, dried over anhydrous MgSO_4 , filtered, and concentrated to give a faint green liquid. The desired product (**31d**) was precipitated by trituration with cold pentanes and isolated in 82% yield as white crystals (51.0 mg, 0.26 mmol). Mp 116–118 °C; ^1H -NMR (600 MHz, CDCl_3) δ 8.25 (d, $J = 4.7$ Hz, 1 H), 7.64–7.58 (m, 1 H), 7.41 (d, $J = 7.0$ Hz, 2 H), 7.35 (t, $J = 7.3$ Hz, 2 H), 7.32–7.28 (m, 1 H), 7.13 (d, $J = 8.5$ Hz, 1 H), 6.83 (dd, $J = 7.0, 5.3$ Hz, 1 H), 4.84 (s, 2 H); ^{13}C -NMR (150 MHz, CDCl_3) δ 162.1, 146.9, 137.8, 137.0, 129.0, 128.4, 127.5, 116.3, 109.7, 58.7; HRMS-ESI (m/z): $[\text{M}+\text{H}]^+$ calcd. for $\text{C}_{12}\text{H}_{13}\text{N}_2\text{O}$: 201.1022, found 201.1019; IR (neat): 3120.2 (br), 3068.3, 3029.9, 1591.2, 1432.2, 1213.4, 986.2 cm^{-1} ; HPLC retention time 6.30 min.

***N*-Benzylpyridin-2-amine (32):** Compound **31d** (2.7 mg, 0.013 mmol) was dissolved in 3 mL of MeOH in a round bottom flask. The flask was charged with 10% Pd-C (0.2 mg) and sealed under argon. The flask was flushed several times with hydrogen gas using intermediate vacuum evacuations. The mixture was then left to stir at rt under a hydrogen atmosphere (1 atm). After 30 min, no starting material (**31d**) was detected by TLC (20% EtOAc in hexanes). The flask was flushed with argon and the mixture was vacuum filtered through celite. Evaporation of the MeOH gave pure product (**32**) in 97% yield as a white solid (2.4 mg, 0.013 mmol). ^1H -NMR (300 MHz, CDCl_3) δ ppm 8.04 (ddd, $J = 5.0, 2.0, 1.0$ Hz, 1 H), 7.40–7.16 (m, 5 H), 6.53 (ddd, $J = 7.1, 5.0, 0.8$ Hz, 1 H), 6.31 (dt, $J = 8.4, 1.1$ Hz, 1 H), 4.87 (br s, NH, 1 H), 4.44 (d, $J = 5.8$ Hz, 2 H); HRMS-ESI (m/z): $[\text{M}+\text{H}]^+$ calcd. for $\text{C}_{12}\text{H}_{13}\text{N}_2$: 185.1073, found 185.1066; HPLC retention time 6.42 min. Data was consistent with material from commercial sources (Sigma- Aldrich Co.).

Typical procedure for the O-acetylation of *N*-alkyl-*N*-(pyridin-2-yl)hydroxylamines

***O*-Acetyl-*N*-benzyl-*N*-(pyridin-2-yl)hydroxylamine (33):** Compound **31d** (8.0 mg, 0.04 mmol), Ac_2O (4.9 mg, 0.05 mmol), $i\text{Pr}_2\text{EtN}$ (7.8 mg, 0.06 mmol), and catalytic DMAP (1.0 mg, 0.01 mmol) were dissolved in 4 mL of anhydrous CH_2Cl_2 , respectively. After 12 h, no starting material (**31d**) was detected by TLC (20% EtOAc in hexanes). The CH_2Cl_2 was evaporated and the crude product was purified by column chromatography (0.25×5 in silica gel; 10%–20% EtOAc in hexanes) to give the desired product (**33**) in 72% yield as a clear, faint yellow oil (7.0 mg, 0.03 mmol). ^1H -NMR (300 MHz, CDCl_3) δ 8.36 (ddd, $J = 4.9, 1.7, 0.8$ Hz, 1 H), 7.65–7.57 (m, 1 H), 7.42–7.25 (m, 5 H), 6.94 (ddd, $J = 7.2, 4.9, 0.8$ Hz, 1 H), 6.80 (dt, $J = 8.5, 0.9$ Hz, 1 H), 5.01 (s, 2 H), 2.04 (s, 3 H); ^{13}C -NMR (75 MHz, CDCl_3) δ 176.3, 160.4, 147.7, 137.9, 135.9, 129.3, 128.3, 127.6, 117.8, 109.9, 57.4, 18.8; HRMS-ESI (m/z): $[\text{M}+\text{H}]^+$ calcd. for $\text{C}_{14}\text{H}_{15}\text{N}_2\text{O}_2$: 243.1128, found 243.1137; IR (neat): 3063.1, 3031.2, 3008.4, 1780.6, 1590.0, 1467.2, 1434.7, 1184.1 cm^{-1} ; HPLC retention time 7.19 min.

(±) 5-Bromo-N-((1S/R,4S/R)-4-methoxycyclohex-2-enyl)pyridin-2-amine (34): This compound was prepared following a general method reported previously.⁴⁸ Activated zinc (65 mg, 1.00 mmol) was added to a solution of Cp₂TiCl₂ (124.0 mg, 0.50 mmol) in 3 mL of anhydrous THF in a flame-dried round bottom flask purged with argon. This mixture was stirred at rt for 45 min. The reaction mixture changed color from dark red to olive green. The mixture was cooled to -30 °C and a solution of **7b** (60.0 mg, 0.20 mmol) in 2 mL of MeOH was added dropwise over 3 min. The mixture was stirred for 1 h while the bath temperature was maintained between -10 and -30 °C. The mixture was warmed to rt and partitioned between satd. aq. K₂CO₃ (5 mL) and EtOAc (15 mL). The organic layer was separated and filtered through a Whatman glass microfiber filter (type GF/F). The aq. layer was extracted with EtOAc (2 × 10 mL) and the separated organic layer was filtered through a Whatman glass microfiber filter (type GF/F) each time. The combined, filtered organics were dried over Na₂SO₄, filtered through a Whatman glass microfiber filter (type GF/F), and concentrated. The crude product was purified by column chromatography (0.5 × 6 in silica gel; 25% EtOAc in hexanes) to give the desired product (**34**) in 73% yield as a white solid (41.6 mg, 0.15 mmol). Mp 50–52 °C; ¹H-NMR (600 MHz, DMSO-*d*₆) δ 8.01 (dd, *J* = 2.5, 0.4 Hz, 1 H), 7.48 (dd, *J* = 8.9, 2.5 Hz, 1 H), 6.74 (d, *J* = 6.5 Hz, 1 H), 6.51 (dd, *J* = 8.9, 0.7, 1 H), 5.86–5.81 (m, 1 H), 5.74–5.70 (m, 1 H), 3.99–3.93 (m, 1 H), 3.71 (td, *J* = 4.4, 2.0 Hz, 1 H), 3.28 (s, 3 H), 2.12–2.05 (m, 2 H), 1.89–1.81 (m, 1 H), 1.55–1.46 (m, 1 H); ¹³C-NMR (150 MHz, DMSO-*d*₆) δ 157.1, 147.4, 138.8, 129.9, 126.3, 110.7, 104.7, 77.2, 55.4, 49.1, 25.7, 23.2; HRMS-ESI (*m/z*): [M+H]⁺ calcd. for C₁₂H₁₆BrN₂O: 283.0441, found 283.0455; IR (neat): 3301.6 (br), 3161.9, 3131.0, 3071.3, 3032.0, 3001.8, 1593.8, 1498.8, 1099.3, 1085.8 cm⁻¹; HPLC retention time 7.48 min.

N-(4-Methoxybenzyloxy)-N-benzyl(pyridin-2-yl)methanamine (38): Compound **29d** (36.0 mg, 0.15 mmol), 2-(bromomethyl)pyridine hydrobromide (56.2 mg, 0.22 mmol), and *i*Pr₂EtN (0.10 mL, 0.57 mmol) were dissolved in 6 mL of anhydrous CH₃CN, respectively. This clear, red solution was heated to 50 °C (oil bath temperature) overnight. After 17 h, only trace starting material (**29d**) was detected by TLC (33% EtOAc in hexanes). The reaction mixture was cooled to rt and the CH₃CN was evaporated under reduced pressure. The resulting material was purified by silica gel column chromatography (0.75 × 4 in silica gel; 20%–40% EtOAc in hexanes) to give the desired product (**38**) in 44% yield as a clear, faint yellow oil (22.0 mg, 0.07 mmol). ¹H-NMR (600 MHz, CDCl₃) δ 8.61 (ddd, *J* = 4.9, 1.8, 0.9 Hz, 1 H), 7.67 (td, *J* = 7.6, 1.8 Hz, 1 H), 7.47–7.43 (m, 3 H), 7.37–7.33 (m, 2 H), 7.33–7.28 (m, 1 H), 7.21 (ddd, *J* = 7.6, 4.9, 1.3 Hz, 1 H), 6.88–6.84 (m, 2 H), 6.76–6.73 (m, 2 H), 4.15 (s, 2 H), 4.07 (s, 2 H), 3.96 (s, 2 H), 3.76 (s, 3 H); ¹³C-NMR (150 MHz, CDCl₃) δ 159.2, 157.8, 149.2, 137.4, 136.1, 130.5, 130.0, 129.1, 128.1, 127.3, 124.2, 122.2, 113.5, 75.4, 64.7, 63.2, 55.2; HRMS-ESI (*m/z*): [M+H]⁺ calcd. for C₂₁H₂₃N₂O₂: 335.1754, found 335.1738; IR (neat): 3062.3, 3031.4, 3007.4, 1611.97, 1588.8, 1513.3, 1247.4, 1032.5 cm⁻¹; HPLC retention time 8.81 min.

Microbiology

General materials and methods—All liquids and media were sterilized by autoclaving (121 °C, 15 min) before use. All aq. solutions and media were prepared using distilled, deionized, and filtered water (Millipore Milli-Q Advantage A10 Water Purification System). Luria broth (LB) was purchased from VWR. Mueller-Hinton No. 2 broth (MHII broth; cation adjusted) was purchased from Sigma-Aldrich (St. Louis, MO). Mueller-Hinton No. 2 agar (MHII agar; HiMedia Laboratories) was purchased from VWR. McFarland BaSO₄ turbidity standards were purchased from bioMerieux, Inc. Sterile plastic petri dishes (145 mm × 20 mm; Greiner Bio-One) were purchased from VWR. Ciprofloxacin was purchased from Sigma-Aldrich (St. Louis, MO). Amphotericin B was purchased from Amresco (Solon,

OH). All test organisms used in this work were from sources given in the supporting information (Table S3).

Antibiotic susceptibility testing by the agar diffusion method—Antibacterial activity of the compounds was determined by a modified Kirby-Bauer agar diffusion assay.⁵⁰ Overnight cultures of test organisms were grown in LB broth for 18–24 h and standard suspensions of 1.5×10^6 CFU/mL were prepared in saline solution (0.9% NaCl) according to a 0.5 BaSO₄ McFarland Standard.⁷⁶ Each standardized suspension (0.1 mL) was added to 34 mL of sterile, melted MHII agar tempered to 47–50 °C. After gentle mixing, the inoculated agar media was poured into a sterile plastic petri dish (145 mm × 20 mm) and allowed to solidify near a flame with the lid cracked for ~30 min. Wells of 9.0 mm diameter were cut from the petri dish agar and filled with exactly 50 µL of the test sample solution. The petri dish was incubated at 37 °C for 18–24 h and the inhibition zone diameters were measured (mm) with an electronic caliper after 24–48 h.

Antibiotic susceptibility testing by the broth microdilution method—Antibacterial activity of the compounds was determined by measuring their minimum inhibitory concentrations (MIC₉₀'s) using the broth microdilution method according to the Clinical and Laboratory Standards Institute (CLSI, formerly the NCCLS) guidelines.⁵² Each well of a 96-well microtiter plate was filled with 50 µL of sterile MHII broth. Each test compound was dissolved in DMSO making a 20 mM solution, then diluted with sterile MHII broth to 512 µM. Exactly 50 µL of the compound solution was added to the first well of the microtiter plate and 2-fold serial dilutions were made down each row of the plate. Exactly 50 µL of bacterial inoculum (5×10^5 CFU/mL in MHII broth) was then added to each well giving a total volume of 100 µL/well and a final compound concentration gradient of 128 µM–0.0625 µM. The plate was incubated at 37 °C for 18 h and then each well was examined for bacterial growth. The MIC₉₀ was recorded as the lowest compound concentration (µM) required to inhibit 90% of bacterial growth as judged by turbidity of the culture media relative to a row of wells filled with a DMSO standard. Ciprofloxacin was included in a control row at a concentration gradient of 32 µM–0.0156 µM.

Supplementary Material

Refer to Web version on PubMed Central for supplementary material.

Acknowledgments

We gratefully acknowledge the use of NMR facilities provided by the Lizzadro Magnetic Resonance Research Center at The University of Notre Dame (UND) and the mass spectrometry services provided by The UND Mass Spectrometry & Proteomics Facility (Mrs. N. Sevova, Dr. W. Boggess, and Dr. M. V. Joyce; supported by the National Science Foundation under CHE-0741793). We thank Mrs. Patricia A. Miller (UND) for anticancer testing and assistance with antibacterial susceptibility testing. We thank Dr. Ute Mollmann (HKI) for antibacterial testing against the resistant strains *S. aureus* 134/94 (MRSA) and *E. faecalis* 1528 (VRE) and for many helpful discussions. We thank Dr. Viktor Krchňak (UND) for assistance with analytical and preparative HPLC and for helpful discussions. TAW gratefully acknowledges The UND Chemistry-Biochemistry-Biology Interface (CBBI) Program funded by NIH (T32GM075762) for three years of fellowship support. TAW also thanks The UND Department of Chemistry and Biochemistry (Grace Fellowship), the Center for Environmental Science and Technology (CEST), and Bayer for additional fellowship support. BY acknowledges a Reilly Graduate Fellowship and JRR acknowledges a College of Science Summer Undergraduate Research Fellowship (COS-SURF), both sponsored by UND. We acknowledge The University of Notre Dame and the NIH (GM 075855) for supporting this work.

References

1. Boucher HW, Talbot GH, Bradley JS, Edwards JE Jr, Gilbert D, Rice LB, Scheld M, Spellberg B, Bartlett J. Bad Bugs, No Drugs: No ESKAPE! An Update from the Infectious Diseases Society of America. *Clinical Infectious Diseases*. 2009; 48:1–12. [PubMed: 19035777]
2. Spellberg B, Guidos R, Gilbert D, Bradley J, Boucher HW, Scheld WM, Bartlett JG, Edwards J Jr. The Epidemic of Antibiotic-Resistant Infections: A Call to Action for the Medical Community from the Infectious Diseases Society of America. *Clinical Infectious Diseases*. 2008; 46:155–164. [PubMed: 18171244]
3. [Accessed April 4, 2011.] Bad Bugs, No Drugs As Antibiotic Discovery Stagnates, A Public Health Crisis Brews. Infectious Disease Society of America (ISDA) Report. July. 2004 Available at: <www.idsociety.org>
4. Laxminarayan, R.; Malani, A. Resources for the Future. Washington, DC: 2007. Extending the Cure: Policy Responses to the Growing Threat of Antibiotic Resistance; p. 1-175.
5. Fischback MA, Walsh CT. Antibiotics for Emerging Pathogens. *Science*. 2009; 325:1089–1093. [PubMed: 19713519]
6. Testero, SA.; Fisher, JF.; Mobashery, S. β -Lactam Antibiotics. Burger's Medicinal Chemistry. In: Abraham, DJ.; Rotella, DP., editors. Drug Discovery and Development. 7. Wiley; Hoboken, NJ: 2010. p. 259-404.
7. Silver LL. Multi-Targeting by Monotherapeutic Antibacterials. *Nat Rev Drug Discovery*. 2007; 6:41–55.
8. Schreiber SL. Small Molecules: The Missing Link in the Central Dogma. *Nat Chem Biol*. 2005; 1:64–66. [PubMed: 16407997]
9. Amer FA, El-Beheedy EM, Mohtady HA. New Targets for Antibacterial Agents. *Biotechnol Mol Biol Rev*. 2008; 3:46–57.
10. Miller JR, Dunham S, Mochalkin I, Banotai C, Bowman M, Buist S, Dunkle B, Hanna D, Harwood HJ, Huband MD, Kamovsky A, Kuhn M, Limberakis C, Liu JY, Mehrens S, Mueller WT, Narasimhan L, Ogden A, Ohren J, Prasad JNVN, Shelly JA, Skerlos L, Sulavik M, Thomas VH, VanderRoest S, Wang L, Wang Z, Whitton A, Zhu T, Stover CK. A Class of Selective Antibacterials Derived from a Protein Kinase Inhibitor Pharmacophore. *Proc Nat Acad Sci US A*. 2009; 106:1737–1742.
11. Walsh CT, Fischbach MA. Repurposing Libraries of Eukaryotic Protein Kinase Inhibitors for Antibiotic Discovery. 2009; 106:1689–1690.
12. Silver LL. Are Natural Products Still the Best Source for Antibacterial Discovery? The Bacterial Entry Factor. *Expert Opin Drug Discovery*. 2008; 3:487–500.
13. O'Shea R, Moser HE. Physicochemical Properties of Antibacterial Compounds: Implications in Drug Discovery. *J Med Chem*. 2008; 51:2871–2878. [PubMed: 18260614]
14. For reviews of FBDD see: (a) Murray CW, Rees DC. The Rise of Fragment-Based Drug Discovery. *Nat Chem*. 2009; 1:187–192. [PubMed: 21378847] (b) Congreve M, Chessari G, Tisi D, Woodhead AJ. Recent Developments in Fragment-Based Drug Discovery. *J Med Chem*. 2008; 51:3661–3680. [PubMed: 18457385] (c) Erlanson DA, McDowell RS, O'Brien T. Fragment-Based Drug Discovery. *J Med Chem*. 2004; 47:3463–3482. [PubMed: 15214773]
15. For successful application of FBDD for antibacterial discovery see: (a) Mochalkin I, Miller JR, Narasimhan L, Thanabal V, Erdman P, Cox PB, Prasad JNVN, Lightle S, Huband MD, Stover CK. Discovery of Antibacterial Biotin Carboxylase Inhibitors by Virtual Screening and Fragment-Based Approaches. *ACS Chem Biol*. 2009; 4:473–483. [PubMed: 19413326] (b) Waldrop GL. Smaller is Better for Antibiotic Discovery. *ACS Chem Biol*. 2009; 4:397–399. [PubMed: 19537754]
16. For successful application of computational structure-based design methods for antibacterial discovery see: Shen Y, Liu J, Estiu G, Isin B, Ahn YY, Lee DS, Barabasi AL, Kapatral V, Wiest O, Oltvai ZN. Blueprint for Antimicrobial Hit Discovery Targeting Metabolic Networks. *Proc Nat Acad Sci US A*. 2010; 107:1082–1087.
17. For successful applications of target-based HTS for antibacterial discovery see: (a) Jarvest RL, Berge JM, Berry V, Boyd HF, Brown MJ, Elder JS, Forrest AK, Fosberry AP, Gentry DR, Hibbs

- MJ, Jaworski DD, O'Hanlon PJ, Pope AJ, Rittenhouse S, Sheppard RJ, Slater-Radosti C, Worby A. Nanomolar Inhibitors of *Staphylococcus aureus* Methionyl tRNA Synthetase with Potent Antibacterial Activity Against Gram-Positive Pathogens. *J Med Chem.* 2002; 45:1959–1962. [PubMed: 11985462] (b) Payne DJ, Miller WH, Berry V, Brosky J, Burgess WJ, Chen E, DeWolf WE Jr, Fosberry AP, Greenwood R, Head MS, Heerding DA, Janson CA, Jaworski DD, Keller PM, Manley PJ, Moore TD, Newlander KA, Pearson S, Polizzi BJ, Qiu X, Rittenhouse SF, Slater-Radosti C, Salyers KL, Seefeld MA, Smyth MG, Takata DT, Uzinskas IN, Vaidya K, Wallis NG, Winram SB, Yuan CCK, Huffman WF. Discovery of a Novel and Potent Class of FabI-Directed Antibacterial Agents. *Antimicrob Agents Chemother.* 2002; 46:3118–3124. [PubMed: 12234833] (c) Fan F, Yan K, Wallis NG, Reed S, Moore TD, Rittenhouse SF, DeWolf WE Jr, Huang J, McDevitt D, Miller WH, Seefeld MA, Newlander KA, Jakas DR, Head MS, Payne DJ. Defining and Combating the Mechanisms of Triclosan Resistance in Clinical Isolates of *Staphylococcus aureus*. *Antimicrob Agents Chemother.* 2002; 46:3343–3347. [PubMed: 12384334]
18. Walsh DP, Chang YT. Chemical Genetics. *Chem Rev.* 2006; 106:2476–2530. [PubMed: 16771457]
 19. Payne DJ, Gwynn MN, Holmes DJ, Pompliano DL. Drugs for Bad Bugs: Confronting the Challenges of Antibacterial Discovery. *Nat Rev Drug Discovery.* 2007; 6:29–40.
 20. As of 2007, only one combinatorial chemistry-derived compound has been approved by the FDA: Newman DJ, Cragg GM. Natural Products as Sources of New Drugs over the Last 25 Years. *J Nat Prod.* 2007; 70:461–477. [PubMed: 17309302]
 21. Schreiber SL. Target-Oriented and Diversity-Oriented Organic Synthesis in Drug Discovery. *Science.* 2000; 287:1964–1969. [PubMed: 10720315]
 22. Burke MD, Schreiber SL. A Planning Strategy for Diversity-Oriented Synthesis. *Ang Chem, Int Ed.* 2004; 43:46–58.
 23. For application of DOS for antibacterial discovery and definitions of structural diversity see: Galloway WRJD, Bender A, Welch M, Spring DR. The Discovery of Antibacterial Agents Using Diversity-Oriented Synthesis. *Chem Comm.* 2009:2446–2462. [PubMed: 19532856]
 24. Yang B, Miller MJ. Regio- and Stereoselective Indium Triflate-Mediated Nucleophilic Ring-Opening Reactions of 3-Aza-2-oxabicyclo[2.2.1]hept-5-ene and -[2.2.2]oct-5-ene Systems. *J Org Chem.* 2009; 74:7990–7993. [PubMed: 19754105]
 25. Yang B, Miller MJ. Regio- and Stereochemically Controlled Formation of Hydroxamic Acids From Indium Triflate-Mediated Nucleophilic Ring-Opening Reactions with Acylnitroso-Diels-Alder Adducts. *Tetrahedron Lett.* 2010; 51:889–891. [PubMed: 20209116]
 26. Yang B, Miller MJ. Iminonitroso Ene Reactions: Experimental Studies on Reactivity, Regioselectivity, and Enantioselectivity. *Tetrahedron Lett.* 2010; 51:328–331. [PubMed: 20161491]
 27. Vogt PF, Miller MJ. Development and Applications of Amino Acid-Derived Chiral Acylnitroso Hetero Diels-Alder Reactions. *Tetrahedron.* 1998; 54:1317–1348.
 28. Li F, Yang B, Miller MJ, Zajicek J, Noll BC, Mollmann U, Dahse HM, Miller PA. Iminonitroso Diels-Alder Reactions for Efficient Derivatization and Functionalization of Complex Diene-Containing Natural Products. *Org Lett.* 2007; 9:2923–2926. [PubMed: 17602642]
 29. Krchňak V, Waring KR, Noll BC, Moellmann U, Dahse HM, Miller MJ. Evolution of Natural Product Scaffolds by Acyl- and Arylnitroso Hetero-Diels-Alder Reactions: New Chemistry on Piperine. *J Org Chem.* 2008; 73:4559–4567. [PubMed: 18489157]
 30. Yang B, Miller PA, Mollmann U, Miller MJ. Syntheses and Biological Activity Studies of Novel Sterol Analogs from Nitroso Diels-Alder Reactions of Ergosterol. *Org Lett.* 2009; 11:2828–2831. [PubMed: 19552465]
 31. Bodnar B, Miller MJ. The Nitrosocarbonyl Hetero-Diels-Alder Reaction as a Useful Tool for Organic Syntheses. *Ang Chem Int Ed.* 2011; 50:5630–5647.
 32. Krchňak V, Zajiček J, Miller PA, Miller MJ. Selective Molecular Sequestration with Concurrent Natural Product Functionalization and Derivatization: From Crude Natural Product Extracts to a Single Natural Product Derivative in One Step. 2011 To be submitted for publication.

33. Krchňak V, Moellmann U, Dahse HM, Miller MJ. Solid-Supported Nitroso Hetero-Diels-Alder Reactions. 3. Acid-Mediated Transformation of Cycloadducts by Scission of the Oxazine C-O Bonds. *J Comb Chem.* 2008; 10:112–117. [PubMed: 18067270]
34. Credito K, Lin G, Ednie LM, Appelbaum PC. Antistaphylococcal Activity of LBM415, a New Peptide Deformylase Inhibitor, Compared with Those of Other Agents. *Antimicrob Agents Chemother.* 2004; 48:4033–4036. [PubMed: 15388473]
35. Chen DZ, Patel DV, Hackbarth CJ, Wang W, Dreyer G, Young DC, Margolis PS, Wu C, Ni ZJ, Trias J, White RJ, Yuan Z. Actinonin, a Naturally Occurring Antibacterial Agent, Is a Potent Deformylase Inhibitor. *Biochemistry.* 2000; 39:1256–1262. [PubMed: 10684604]
36. Mine Y, Kamimura T, Nonoyama S, Nishida M, Goto S, Kuwahara S. *In Vitro* and *In Vivo* Antibacterial Activities of FR-31564, a New Phosphonic Acid Antibiotic. *J Antibiot.* 1980; 33:36–43. [PubMed: 7372548]
37. Onishi HR, Pelak BA, Gerckens LS, Silver LL, Kahan FM, Chen MH, Patchett AA, Galloway SM, Hyland SA, Anderson MS, Raetz CRH. Antibacterial Agents That Inhibit Lipid A Biosynthesis. *Science.* 1996; 274:980–982. [PubMed: 8875939]
38. Woulfe SR, Miller MJ. Heteroatom Activated β -Lactam Antibiotics: Synthesis of Biologically Active Substituted *N*-Oxy-3-amino-2-azetidinones (Oxamazins). *Tetrahedron Lett.* 1984; 25:3293–3296.
39. Muci AR, Buchwald SL. Practical Palladium Catalysts for C-N and C-O Bond Formation. *Top Curr Chem.* 2002; 219:131–209.
40. Hartwig JF. Evolution of a Fourth Generation Catalyst for the Amination and Thioetherification of Aryl Halides. *Acc Chem Res.* 2008; 41:1534–1544. [PubMed: 18681463]
41. Roosenberg JM, Miller MJ. Total Synthesis of the Siderophore Danoxamine. *J Org Chem.* 2000; 65:4833–4838. [PubMed: 10956460]
42. Gebhardt P, Crumbliss AL, Miller MJ, Mollmann U. Synthesis and Biological Activity of Saccharide Based Lipophilic Siderophore Mimetics as Potential Growth Promoters for Mycobacteria. *Biometals.* 2008; 21:41–51. [PubMed: 17390213]
43. Yan L, Kahne D. *p*-Methoxybenzyl Ethers as Acid-Labile Protecting Groups in Oligosaccharide Synthesis. *Synlett.* 1995:523–524.
44. Zhu G, Yang F, Balachandran R, Hook P, Vallee RB, Curran DP, Day BW. Synthesis and Biological Evaluation of Purealin and Analogues as Cytoplasmic Dynein Heavy Chain Inhibitors. *J Med Chem.* 2006; 49:2063–2076. [PubMed: 16539395]
45. Schumann EL, Heinzelman RV, Greig ME, Veldkamp W. Hydroxylamine Chemistry. IV. *O*-Aralkylhydroxylamines. *J Med Chem.* 1964; 7:329–334. [PubMed: 14207837]
46. McKay AF, Garmaise DL, Paris GY, Gelblum S. Bacteriostats. III. Oxyamines and Their Derivatives. *Can J Chem.* 1960; 38:343–358.
47. Wagaw S, Buchwald SL. The Synthesis of Aminopyridines: A Method Employing Palladium-Catalyzed Carbon-Nitrogen Bond Formation. *J Org Chem.* 1996; 61:7240–7241. [PubMed: 11667641]
48. Cesario C, Tardibono LP, Miller MJ. Titanocene(III) Chloride-Mediated Reductions of Oxazines, Hydroxamic Acids, and *N*-Hydroxy Carbamates. *J Org Chem.* 2009; 74:448–451. [PubMed: 19053586]
49. For the original descriptions of the Kirby-Bauer agar diffusion assay see: (a) Bauer AW, Perry DM, Kirby WMM. Single Disc Antibiotic Sensitivity Testing of *Staphylococci*: An Analysis of Technique and Results. *Arch Int Med.* 1959; 104:208–216. (b) Bauer AW, Kirby WMM, Sherris JC, Turck M. Antibiotic Susceptibility Testing by a Standardized Single Disk Method. *Am J Clin Pathol.* 1966; 45:493–496. [PubMed: 5325707]
50. For a specific example general description of the modified Kirby-Bauer agar diffusion assay used in this study see: Afonin S, Glaser RW, Berdichevskaia M, Wadhvani P, Guhrs K-H, Mollmann U, Perner A, Ulrich AS. 4-Fluoro-phenylglycine as a Label for ^{19}F -NMR Structure Analysis of Membrane Associated Peptides. *ChemBioChem.* 2003; 4:1151–1163. [PubMed: 14613106]
51. Ciprofloxacin [package insert]. Bayer HealthCare Pharmaceuticals, Inc; Wayne, NJ: April. 2009 <http://www.univgraph.com/bayer/inserts/ciprotab.pdf>

52. Methods for Dilution Antimicrobial Susceptibility Tests for Bacteria that Grow Aerobically. 8. Villanova, PA, USA: Clinical and Laboratory Standards Institute (CLSI); 2009. approved standard document M07–A7
53. Eaton RW, Ribbons DW. Metabolism of Dibutylphthalate and Phthalate by *Micrococcus* sp. Strain 12B. *J Bacteriol.* 1982; 151:48–57. [PubMed: 7085570]
54. Mukamolova GV, Murzin AG, Salina EG, Demina GR, Kell DB, Kaprelyants AS, Young M. Muralytic Activity of *Micrococcus luteus* Rpf and its Relationship to Physiological Activity in Promoting Bacterial Growth and Resuscitation. *Mol Microbiol.* 2006; 59:84–98. [PubMed: 16359320]
55. Saito Y, Ogura K. Biosynthesis of Menaquinones. Enzymatic Prenylation of 1,4-Dihydroxy-2-Naphthoate by *Micrococcus luteus* Membrane Fractions. *J Biochem.* 1981; 89:1445–1452. [PubMed: 7275947]
56. Garcia-Lopez, M–L.; Santos, J–A.; Otero, A. *Micrococcus*. In: Robinson, RK.; Batt, CA.; Patel, PD., editors. *Encyclopedia of Food Microbiology*. Vol. 2. Academic Press; San Diego, CA: 2000. p. 1344–1350.
57. Friedman M, Buick R, Elliott CT. Antimicrobial Activities of Plant Compounds Against Antibiotic-Resistant *Micrococcus luteus*. *Int J Antimicrob Agents.* 2006; 28:151–158. [PubMed: 16815688]
58. Smith KJ, Neafie R, Yeager J, Skelton HG. *Micrococcus* folliculitis in HIV-1 Disease. *Br J Dermatol.* 1999; 141:558–561. and references therein. [PubMed: 10583069]
59. Yang S, Sugawara S, Monodane T, Nishijima M, Adachi Y, Akashi S, Miyake K, Hase S, Takada H. *Micrococcus luteus* Teichuronic Acids Activate Human and Murine Monocyte Cells in a CD14– and Toll-Like Receptor 4-Dependent Manner. *Infect Immun.* 2001; 69:2025–2030. and references therein. [PubMed: 11254554]
60. For recent examples of selective antibacterial agents see: (a) Liu CI, Liu GY, Song Y, Yin F, Hensler ME, Jeng WY, Nizet V, Wang AHJ, Oldfield E. A Cholesterol Biosynthesis Inhibitor Blocks *Staphylococcus aureus* Virulence. *Science.* 2008; 319:1391–1394. [PubMed: 18276850] (b) Haydon DJ, Stokes NR, Ure R, Galbraith G, Bennett JM, Brown DR, Baker PJ, Barynin VV, Rice DW, Sedelnikova SE, Heal JR, Sheridan JM, Aiwale ST, Chauhan PK, Srivastava A, Taneja A, Collins I, Errington J, Czaplowski LG. An Inhibitor of FtsZ with Potent and Selective Anti-Staphylococcal Activity. *Science.* 2008; 321:1673–1675. [PubMed: 18801997]
61. Adam W, Krebs O. The Nitroso Ene Reaction: A Regioselective and Stereoselective Allylic Nitrogen Functionalization of Mechanistic Delight and Synthetic Potential. *Chem Rev.* 2003; 103:4131–4146. [PubMed: 14531720]
62. Hwu JR, Tsay S–C, Chen B–L, Patel HV, Chou C–T. *N*-Arylalkyl-*N*-phenylhydroxylamines as Novel Photo-Induced DNA-Cleaving Agents. *J Chem Soc, Chem Commun.* 1994:1427–1428.
63. Kovacic P, Somanathan R. Novel, Unifying Mechanism for Aromatic Primary-Amines (Therapeutics, Carcinogens and Toxins): Electron Transfer, Reactive Oxygen Species, Oxidative Stress and Metabolites. *Med Chem Comm.* 2011; 2:106–112.
64. Yang B, Lin W, Krchňak V, Miller MJ. Retro Iminonitroso Diels-Alder Reactions: Interconversion of Nitroso Cycloadducts. *Tetrahedron Lett.* 2009; 50:5879–5883. [PubMed: 20161032]
65. For examples of *N*-2-pyridylhydroxylamine metal chelation see: (a) Okazawa A, Hashizume D, Ishida T. Ferro- and Antiferromagnetic Coupling Switch Accompanied by Twist Deformation Around the Copper(II) and Nitroxide Coordination Bond. *J Am Chem Soc.* 2010; 132:11516–11524. [PubMed: 20669955] (b) Okazawa A, Ishida T. Spin-Transition-Like Behavior on One Side in a Nitroxide-Copper(II)-Nitroxide Triad System. *Inorg Chem.* 2010; 49:10144–10147. [PubMed: 20925369] (c) Osanai K, Okazawa A, Nogami T, Ishida T. Strong Ferromagnetic Exchange Couplings in Copper(II) and Nickel(II) Complexes with a Paramagnetic Tridentate Chelate Ligand, 2,2'-Bipyridin-6-yl *tert*-Butyl Nitroxide. *J Am Chem Soc.* 2006; 128:14008–14009. [PubMed: 17061866] (d) Okazawa A, Nagaichi Y, Nogami T, Ishida T. Magneto-Structure Relationship in Copper(II) and Nickel(II) Complexes Chelated with Stable *tert*-Butyl 5-Phenyl-2-pyridyl Nitroxide and Related Radicals. *Inorg Chem.* 2008; 47:8859–8868. [PubMed: 18729448]
66. For a review on the metal chelation properties of pyridyl oximes see: Milios CJ, Stamatatos TC, Perlepes SP. The Coordination Chemistry of Pyridyl Oximes. *Polyhedron.* 2006; 25:134–194.

67. Kuzuyama T, Shimizu T, Takahashi S, Seto H. Fosmidomycin, a Specific Inhibitor of 1-Deoxy-D-Xylulose-5-Phosphate Reductoisomerase in the Nonmevalonate Pathway for Terpenoid Biosynthesis. *Tetrahedron Lett.* 1998; 39:7913–7916.
68. Haemers T, Wiesner J, Van Poecke S, Goeman J, Henschker D, Beck E, Jomaa H, Van Calenbergh S. Synthesis of α -Substituted Fosmidomycin Analogues as Highly Potent *Plasmodium falciparum* Growth Inhibitors. *Bioorg Med Chem Lett.* 2006; 16:1888–1891. [PubMed: 16439126]
69. Deng L, Endo K, Kato M, Cheng G, Yajima S, Song Y. Structures of 1-Deoxy-D-Xylulose-5-Phosphate Reductoisomerase/Lipophilic Phosphonate Complexes. *ACS Med Chem Lett.* 2011; 2:165–170. [PubMed: 21379374]
70. Yajima S, Hara K, Sanders JM, Yin F, Ohsawa K, Wiesner J, Jomaa H, Oldfield E. Crystallographic Structures of Two Bisphosphonate: 1-Deoxyxylulose-5-Phosphate Reductoisomerase Complexes. *J Am Chem Soc.* 2004; 126:10824–10825. [PubMed: 15339150]
71. Deng L, Sundriyal S, Rubio V, Shi ZZ, Song Y. Coordination Chemistry Based Approach to Lipophilic Inhibitors of 1-Deoxy-D-Xylulose-5-Phosphate Reductoisomerase. *J Med Chem.* 2009; 52:6539–6542. [PubMed: 19888756]
72. Hunter WN. The Non-Mevalonate Pathway of Isoprenoid Precursor Biosynthesis. *J Biol Chem.* 2007; 282:21573–21577. [PubMed: 17442674]
73. Testa CA, Brown MJ. The Methylerythritol Phosphate Pathway and its Significance as a Novel Drug Target. *Curr Pharm Biotechnol.* 2003; 4:248–259. [PubMed: 14529427]
74. Heath RJ, White SW, Rock CO. Lipid Biosynthesis as a Target for Antibacterial Agents. *Prog Lipid Res.* 2001; 40:467–497. [PubMed: 11591436]
75. Taylor EC, Tseng CP, Rampal JB. Conversion of a Primary Amino Group into a Nitroso Group. Synthesis of Nitroso-Substituted Heterocycles. *J Org Chem.* 1982; 4:552–555.
76. Murray, PR.; Baron, EJ.; Pfaller, MA.; Tenover, FC.; Tenover, RH. *Manual of Clinical Microbiology.* 7. American Society for Microbiology; Washington, DC: 1999.

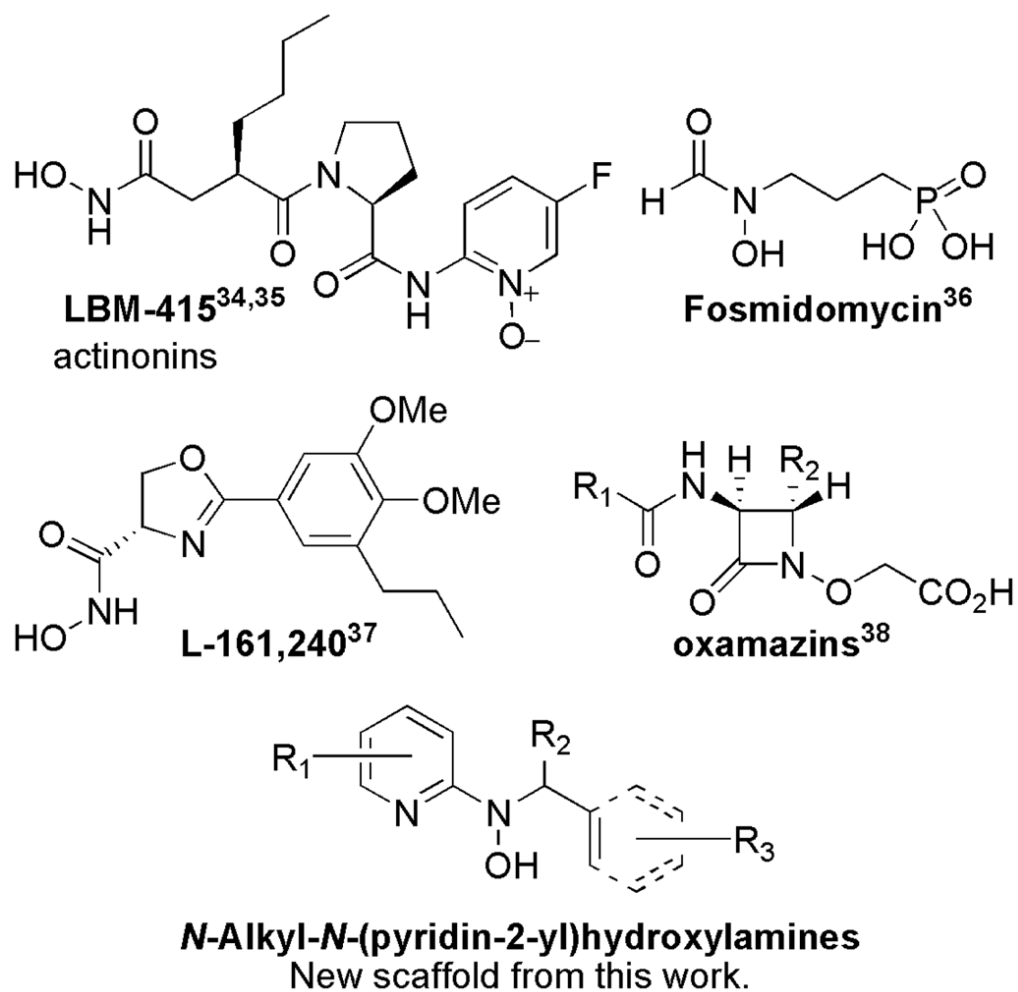
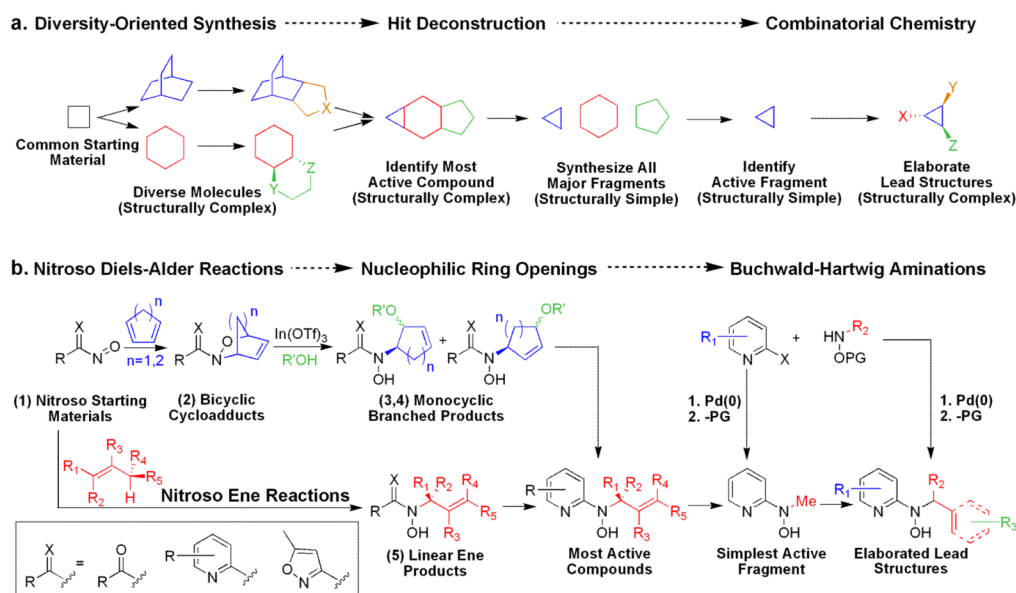


Figure 1. Examples of known antibacterial agents containing an N-O bond and the generic *N*-alkyl-*N*-(pyridin-2-yl)hydroxylamine scaffold from this work.^{34–38}

**Figure 2.**

(a) Generalized DOS and combinatorial chemistry strategy for identifying new biologically active lead scaffolds. (b) Combination strategy of DOS and combinatorial chemistry used for discovering the new antibacterial *N*-alkyl-*N*-(pyridin-2-yl)hydroxylamine scaffold in this work.

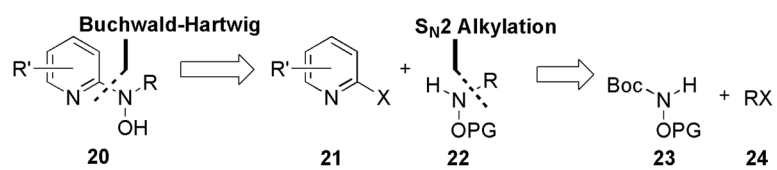


Figure 3.
Retrosynthetic analysis of *N*-alkyl-*N*-(pyridin-2-yl)hydroxylamines (**20**).

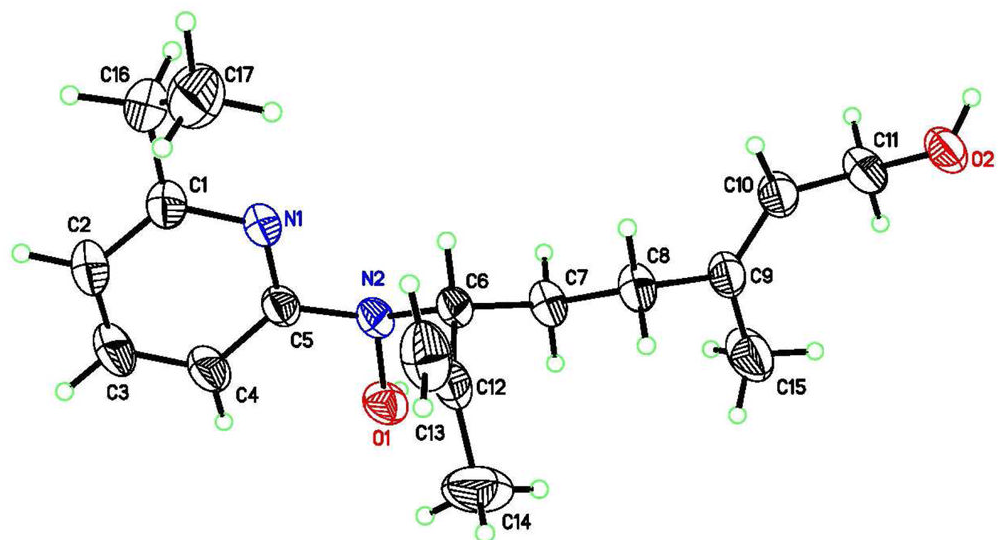


Figure 4.
X-ray diffraction structure of analog **40a** displayed with 50% probability ellipsoids.

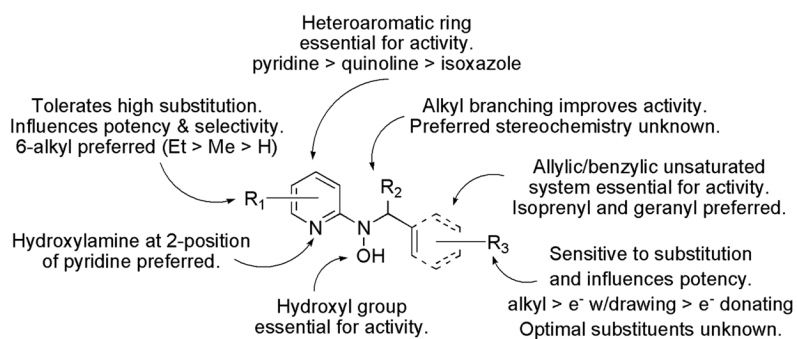


Figure 5. General antibacterial SAR trends for *N*-alkyl-*N*-(pyridin-2-yl)hydroxylamines.

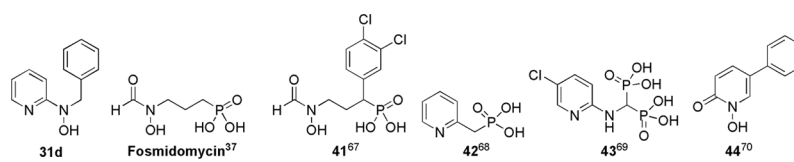
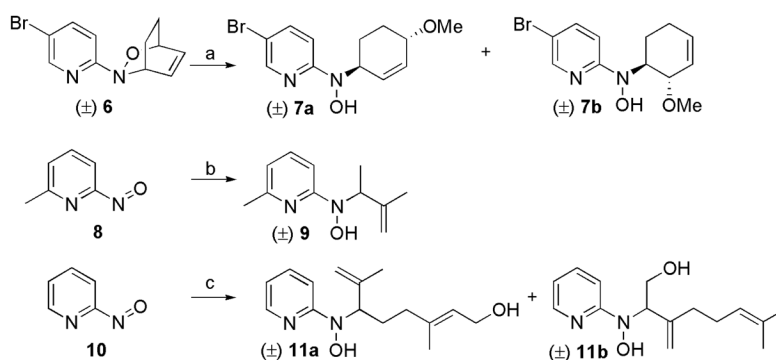
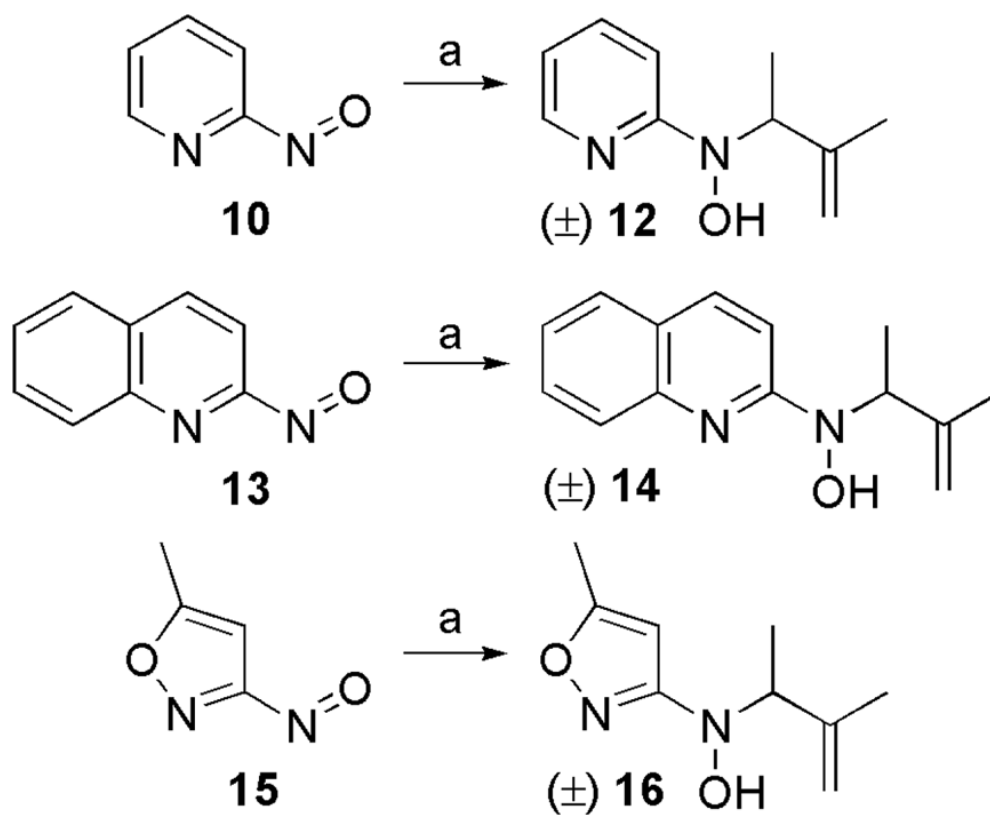


Figure 6. Structural similarities of *N*-benzyl-*N*-(pyridin-2-yl)hydroxylamine (**31d**) to known DXR inhibitors (fosmidomycin and compounds **41–44**).

**Scheme 1.**

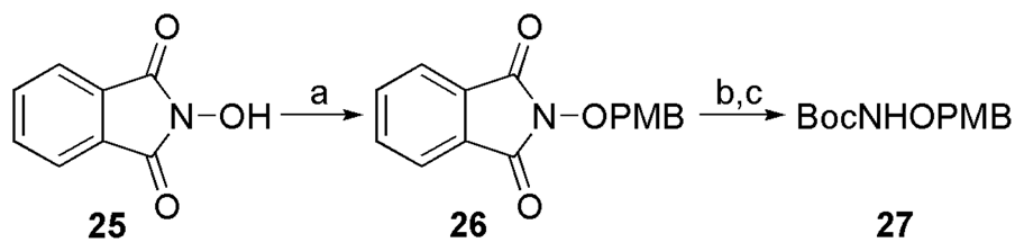
Syntheses of *N*-alkyl-*N*-(pyridin-2-yl)hydroxylamines **7a**, **7b**, **9**, and **11a**, and **11b**.^a

^aReagents and conditions: (a) In(OTf)₃ (1.0 equiv), MeOH, 70 °C, 4 h, 95% (1:1 ratio of **7a**:**7b**); (b) 2-methyl-2-butene (2.0 equiv), CH₂Cl₂, 0 °C–rt, 20 min, 38%; (c) geraniol (2.0 equiv), CH₂Cl₂, 0 °C–rt, 25 min, 71% (72:28 ratio of **11a**:**11b**).

**Scheme 2.**

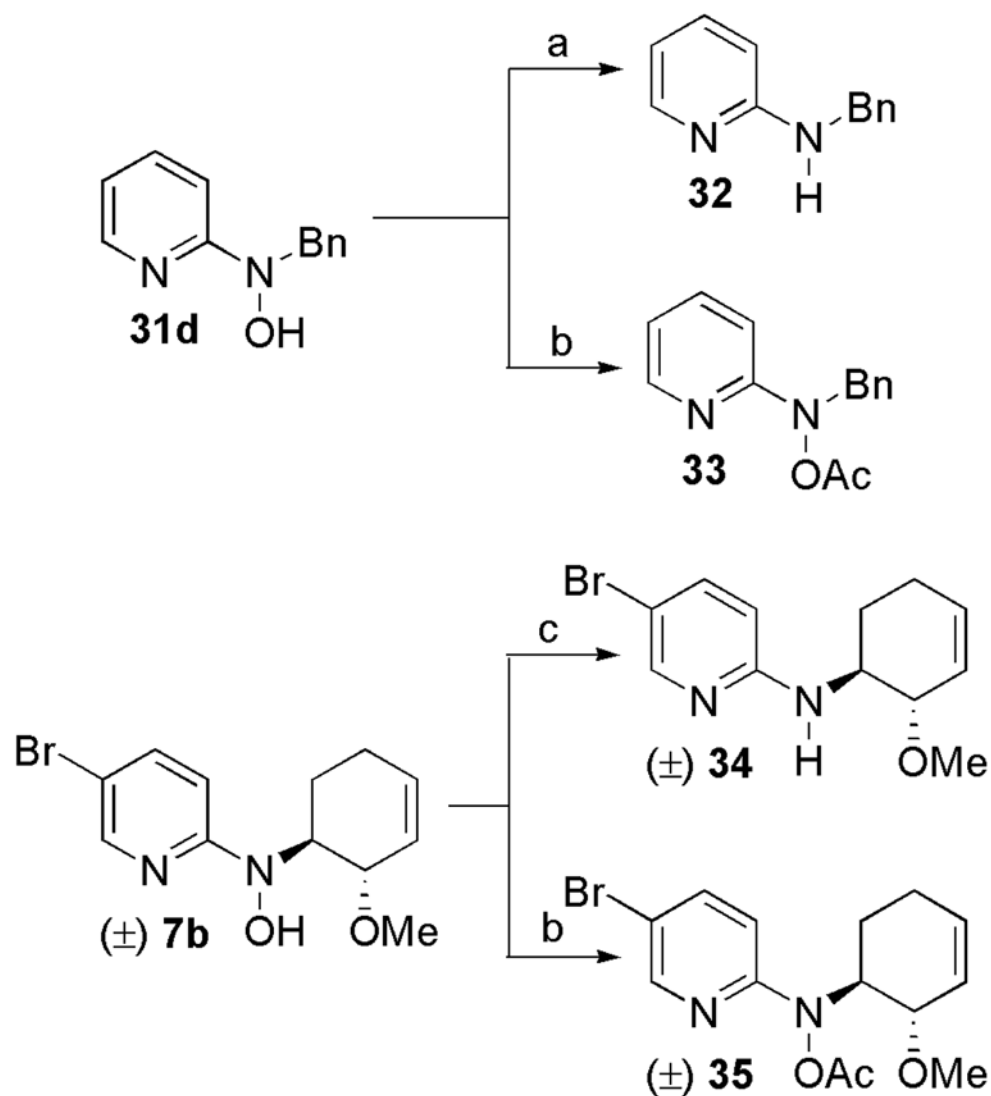
Syntheses of pyridine (**12**), quinoline (**14**), and isoxazole (**16**) hydroxylamine analogs with an isoprenyl side chain.^a

^aReagents and conditions: (a) 2-methyl-2-butene (2.0 equiv), CH_2Cl_2 , 0 °C–rt; 15 min, 48% for **12**; 1 h, 53% for **14**; 10 min, 94% for **16**.

**Scheme 3.**

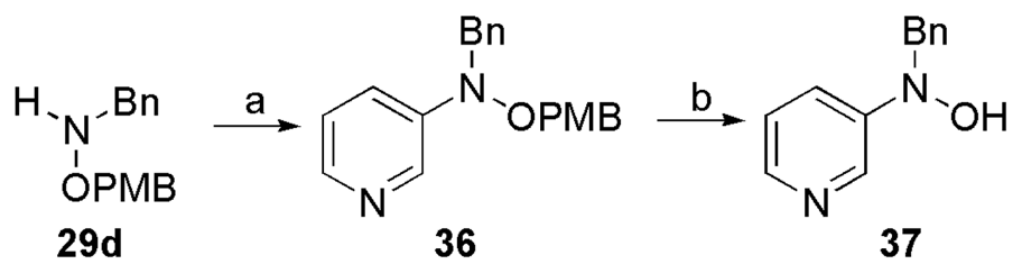
Synthesis of *N*-Boc-*O*-(4-methoxybenzyl)hydroxylamine (BocNHOPMB, 27).^a

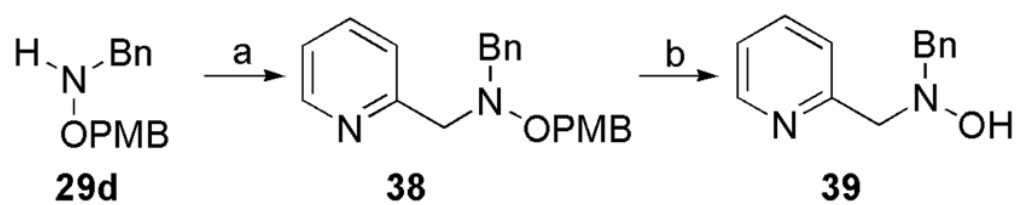
^aReagents and conditions: (a) 4-(methoxybenzyl)chloride, Et₃N, DMF, 90 °C, 1 h, 71%. (b) NH₂NH₂, DMF:MeOH, 60 °C, 10 min. (c) Boc₂O, Et₃N, THF:H₂O, 2 h, 90% (steps b,c).

**Scheme 4.**

Syntheses of N-O reduced analogs (**32** and **34**) and *O*-acetylated analogs (**33** and **35**).^a

^aReagents and conditions: (a) 10% Pd-C, H₂ (1 atm), MeOH, rt, 30 min, 97%. (b) Ac₂O, *i*Pr₂EtN, DMAP, CH₂Cl₂, rt; 12 h, 72% for **33**; 9 h, 94% for **35** (c) Cp₂TiCl₂, Zn, THF/MeOH, -30 °C, 1 h, 73%.

**Scheme 5.**Synthesis of 3-pyridyl analog **37**.^a^aReagents and conditions: (a) 3-bromopyridine, Pd₂(dba)₃, (±) BINAP, NaO^tBu, toluene, 70 °C, 67 h, 36%. (b) TFA, Et₃SiH, CH₂Cl₂, rt, 30 h; then aq. NaHCO₃, 45%.

**Scheme 6.**Synthesis of homologated analog **39**.^a^aReagents and conditions: (a) 2-(bromomethyl)pyridine hydrobromide, *i*Pr₂EtN, CH₃CN, 50 °C, 17 h, 44%. (b) TFA, Et₃SiH, CH₂Cl₂, rt; then aq. NaHCO₃, 5 h, 73%.

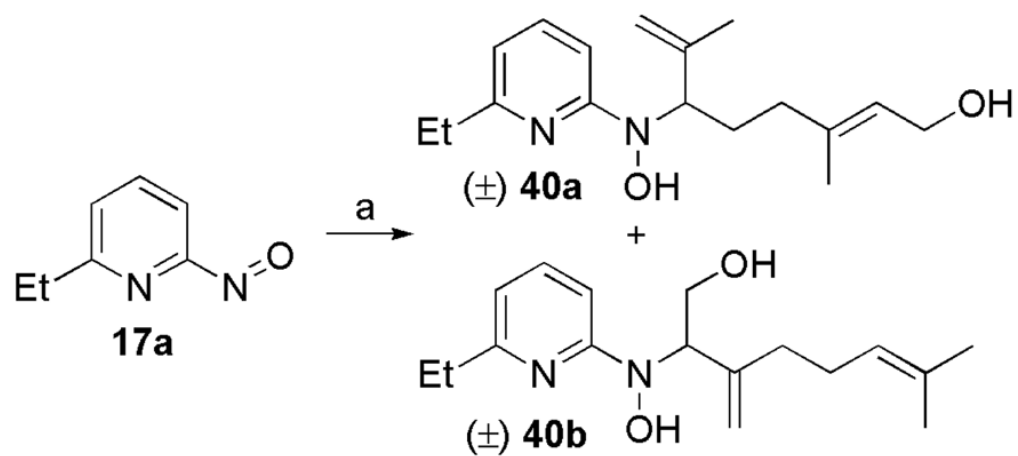
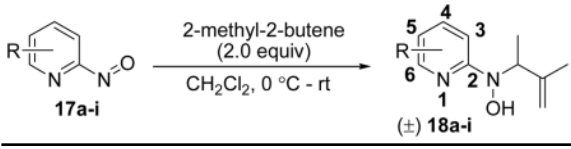
**Scheme 7.**Synthesis of geranyl analogs **40a** and **40b**.^a^aReagents and conditions: (a) geraniol (2.0 equiv), CH₂Cl₂, 0 °C–rt, 30 min, 75% (70:30 ratio of **40a**:**40b**).

Table 1Syntheses of substituted pyridine analogs (**18a-i**) with an isoprenyl side chain.


Comp.	R	Time	% Yield
18a	6-ethyl	30 min	46
18b	4-methyl	30 min	47
18c	3-methyl	9 h	8
18d	5-chloro	30 min	59
18e	5-bromo	10 min	64
18f	5-iodo	1 h	68
18g	3,5-dichloro	1 h	67
18h	5-bromo-6-methyl	30 min	62
18i	3-chloro-5-CF ₃	45 min	75

Table 2Syntheses of pyridine analogs (**19a–c**) with various hydroxylamine side chains.

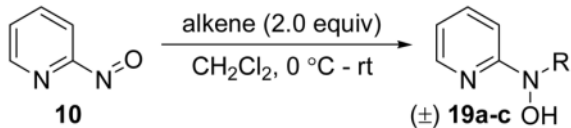
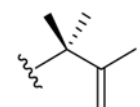
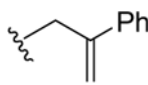
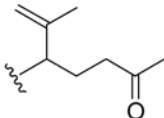
Comp.	R	Time	% Yield
10			
19a		30 min	71
19b		3 h	6
19c		10 min	94

Table 3

Four step syntheses of compounds **28a-i** – **31a-i**.^{a,b}

Comp	Step a		Step b		Step c		Step d	
	Time (h)	% Yield	Time (min)	% Yield	Time (h)	% Yield	Time (h)	% Yield
a	26	91	15	99 ^c	96	77	7	64 ^e
b	5	98 ^d	15	99 ^c	72	51	5	75
c	14	97	15	77	72	39 ^d	12	62
d	6	98 ^d	15	75 ^d	64	63 ^d	5.5	84 ^d
e	10	88 ^d	15	73	60	49	4.5	64 ^d
f	10	87	15	58	66	54	5	55
g	24	50	15	70	70	59	7	60
h	22	98	15	62	96	56	7	81
i	22	86	15	72 ^d	96	53 ^d	19	70
Average	15	88	15	70 ^f	77	56	8	68
Range	5–26	50–98	15	58–77 ^f	60–96	39–77	4.5–19	55–84

^a Reagents and conditions: (a) NaH, RX (alkyl halide), DMF, 0 °C–rt. (b) TFA, CH₂Cl₂, rt; then aq. NaHCO₃. (c) 2-bromopyridine, Pd₂(dba)₃, (±) BINAP, NaOtBu, toluene, 70 °C. (d) TFA, Et₃SiH, CH₂Cl₂, rt; then aq. NaHCO₃.

^b Yields are based on isolated, purified, and characterized material unless otherwise stated and optimal reaction time listed if reactions were replicated.

^c Crude yield.

^d Average of two yields.

^e Average of three yields.

^f Calculated for purified products only.

Table 4

Structure classes and antibiotic activity against *M. luteus* ATCC 10240 in the agar diffusion assay.^{a, b, c}

Structure Type	Class A	Active?	Class B	Active?	Class C	Active?
Nitrosos and Hydroxamic Acids (1)		No ^d		No		No
Diels-Alder Cycloadducts (2)		No		No		No
Ring Opened Compounds (3, 4)		No		Yes ^e		Yes
Ene Products (5)		No		Yes		Yes

^a See supporting information for a complete list of structures and antibacterial data (Tables S1 and S2).^b All compounds were racemic. R = alkyl; O-alkyl; R' = alkyl; halo, carboxyl; R₁, R₂, R₃, R₄, R₅ = alkyl; H; n = 1, 2.^c Exactly 50 μ L of each compound solution (2.0 mM in 10:1 MeOH:DMSO) were added to 9 mm wells in agar media (MHID) inoculated with $\sim 5 \times 10^3$ CFU/mL of *M. luteus* ATCC 10240. Diameters of growth inhibition zones were measured (mm) after incubation at 37 °C for 24 h.⁵⁰^d No: indicates a growth inhibition zone ≤ 14 mm.^e Yes: indicates a growth inhibition zone > 14 mm.

Table 5

Spectrum of antibacterial activity for compounds **7a**, **9**, and **11a** in the agar diffusion assay.^{a,b,c}

Test Organism	Test Compound			ciprofloxacin ^d
	(±) 7a	(±) 9	(±) 11a	
<i>M. luteus</i> ATCC 10240	+++	+++	+++	-
<i>S. aureus</i> SG511	+	+	++	+++
<i>S. aureus</i> 134/94 (MRSA)	+	+	++	+
<i>E. faecalis</i> ATCC 49532	++*	++*	++*	++
<i>E. faecalis</i> 1528 (VRE)	++*	++*	++*	++
<i>B. subtilis</i> ATCC 6633	-	-	+	+++
<i>M. vaccae</i> IMET 10670	+	++	++	+++
<i>E. coli</i> DC0	-	-	-	+++
<i>E. coli</i> DC2	-	-	-	+++
<i>P. aeruginosa</i> 799/WT	-	-	-	+++
<i>P. aeruginosa</i> 799/61	-	-	-	+++
<i>S. salmonicolor</i> 549 (yeast)	-	-	-	++ ^e

^aExactly 50 μ L of each compound solution (2.0 mM in 10:1 MeOH:DMSO) were added to 9 mm wells in agar media (MHII) inoculated with $\sim 5 \times 10^3$ CFU/mL. Diameters of growth inhibition zones were measured (mm) after incubation at 37 °C for 24 h.⁵⁰^bSee supporting information for exact diameters (mm) of inhibition zones (Table S2).^cDiameters of inhibition zones are generalized as follows: +: inhibition zone of 11 – 15 mm; ++: inhibition zone of 16 – 20 mm; +++: inhibition zone of ≥ 21 mm; -: inhibition zone of ≤ 10 mm.^dCiprofloxacin was used as a control at 5 μ g/mL in H₂O.^eAmphotericin B was used as the control (10 μ g/mL in 10:1 DMSO:MeOH) instead of ciprofloxacin.

* Indicates partially unclear inhibition zone.

Table 6

Antibacterial activity of test compounds in the agar diffusion assay^a (diameter of growth inhibition zones given in mm) and the broth microdilution assay^{b,c} (MIC₉₀ values given in μM).

Comp.	Test Organism					
	<i>M. luteus</i> ATCC 10240		<i>S. aureus</i> SG511		<i>E. faecalis</i> ATCC 49532	
	Zone (mm)	MIC ₉₀ (μM)	Zone (mm)	MIC ₉₀ (μM)	Zone (mm)	MIC ₉₀ (μM)
7a	34	4.0	12	>128	16*	>128
7b	34	4.0	18*	≥128	20*	>128
9	48	4.0	12	>128	15*	>128
11a	35	8.0	19	64	20*	>128
12	31	8.0	18	128	22*	>128
14	31	8.0	13	128	13*	>128
16	21	64	0	>128	13*	>128
18a	52	2.0	11	>128	22*	>128
18b	29	4.0	20	128	22*	>128
18c	25	16	10	>128	19*	>128
18d	40	2.0	18	128	21*	≥128
18e	35	4.0	17*	>128	19*	>128
18f	38	2.0	12	>128	19*	>128
18g	27	16.0	0	>128	14*	>128
18h	35	4.0	13	>128	12*	>128
18i	15	128	0	>128	13*	>128
19a	33	4.0	15	128	18*	>128
19b	20	64	19	32	18*	>128
19c	30	16	15*	128	16*	>128
30d	0	>128	0	>128	0	>128
31a	18*	≥128	0	>128	0	>128
31b	13*	>128	0	>128	0	>128
31c	15	128	17*	>128	16*	>128
31d	24	64	18	128	20*	>128
31e	16	128	0	>128	15*	>128
31f	14	>128	0	>128	12*	>128
31g	12*	>128	13	>128	0	>128
31h	16	128	15*	>128	15*	>128
31i	17	128	14*	>128	15*	>128
32	0	>128	0	>128	0	>128

Comp.	Test Organism					
	<i>M. luteus</i> ATCC 10240		<i>S. aureus</i> SG511		<i>E. faecalis</i> ATCC 49532	
	Zone (mm)	MIC ₉₀ (μM)	Zone (mm)	MIC ₉₀ (μM)	Zone (mm)	MIC ₉₀ (μM)
33	20	128	12	>128	11*	>128
34	0	>128	0	>128	0	>128
35	22	32	0	>128	0	>128
37	15*	≥128	16*	>128	0	>128
39	0	>128	0	>128	0	>128
40a	31	2.0	18*	>128	19*	>128
cipro ^d	0	8.0	26	0.5	17	2.0

^a Exactly 50 μL of each compound solution (2.0 mM in 10:1 MeOH:DMSO) were added to 9 mm wells in agar media (MHII) inoculated with ~5×10³ CFU/mL. Diameters of growth inhibition zones were measured (mm) after incubation at 37 °C for 24 h.⁵⁰

^b MIC₉₀ values were determined by the visual end point broth microdilution method following CLSI guidelines.⁵²

^c Each compound was tested in triplicate.

^d Ciprofloxacin was used as a standard at 5 μg/mL in H₂O in the agar diffusion assay.

* Indicates partially unclear inhibition zone.